Microbiology and Infectious Disease

Efficacy and mechanism of action of cipargamin as an antibabesial drug candidate

Reviewed Preprint
v2 • March 18, 2025
Revised by authors

Reviewed Preprint
v1 • September 11, 2024

Hang Li, Shengwei Ji, Nanang R Ariefta, Eloiza May S Galon, Shimaa AES El-Sayed, Thom Do, Lijun Jia, Miako Sakaguchi, Masahito Asada, Yoshifumi Nishikawa, Xin Qin, Mingming Liu, Xuenan Xuan

National Research Center for Protozoan Diseases, Obihiro University of Agriculture Veterinary Medicine, Obihiro, Japan • Department of Veterinary Medicine, Agriculture College of Yanbian University, Yanji, China • College of Veterinary Medicine and Biomedical Sciences, Cavite State University, Indang, Philippines • Department of Biochemistry and Molecular Biology, Faculty of Veterinary Medicine, Mansoura University, Mansoura Egypt • Central Laboratory, Institute of Tropical Medicine (NEKKEN), Nagasaki University, Nagasaki, Japan • School of Basic Medicine, Hubei University of Arts and Science, Xiangyang, China

eLife Assessment

This study presents **valuable** findings with practical and theoretical implications for drug discovery, particularly in the context of repurposing cipargamin CIP for the treatment of Babesia spp. The evidence is **solid** with the methods, data and analyses broadly supporting the claims. The paper will be of great interest to scientists in drug discovery, computational biology, and microbiology

https://doi.org/10.7554/eLife.101128.2.sa3

Abstract

Babesiosis is a disease brought on by intraerythrocytic parasites of the genus *Babesia*. Current chemotherapies are accompanied by side effects and parasite relapse. Therefore, it is crucial to develop highly effective drugs against *Babesia*. Cipargamin (CIP) has shown inhibition against apicomplexan parasites, mainly *Plasmodium* and *Toxoplasma*. This study evaluated the growth-inhibiting properties of CIP against *Babesia* spp. and investigated the mechanism of CIP on *B. gibsoni*. The half inhibitory concentration (IC_{50}) values of CIP against the *in vitro* growth of *B. bovis* and *B. gibsoni* were 20.2 ± 1.4 nM and 69.4 ± 2.2 nM, respectively. CIP significantly inhibited the growth of *B. microti* and *B. rodhaini in vivo*. Resistance was conferred by L921V and L921I mutations in *Bg*ATP4, which reduced the sensitivity to CIP by 6.1- and 12.8-fold. The inhibitory potency of CIP against *Bg*ATP4-associated ATPase activity was moderately reduced in mutant strains, with a 1.3-fold and 2.4-fold decrease in *Bg*ATP4^{L921V} and *Bg*ATP4^{L921I} compared to that of *Bg*ATP4^{WT}, respectively. An *in silico* investigation revealed reductions in affinity for CIP binding to *Bg*ATP4^{L921V} and *Bg*ATP4^{L921I} compared to *Bg*ATP4^{WT}. Resistant strains showed no significant cross-resistance to atovaquone (ATO) or tafenoquine (TQ), with less than a onefold change in IC_{50} values. Combining CIP with TQ effectively eliminated *B. microti* infection in SCID mice, no relapse, and parasite DNA was not detected by qPCR within 90 days post-infection. Our findings reveal

the efficacy of CIP as an anti-babesial agent, its limitations as a monotherapy due to resistance development, and the potential of combination therapy with TQ to overcome resistance and achieve complete parasite clearance.

Introduction

Babesia is an apicomplexan tick-transmitted hemoparasite, which not only impacts the livestock economy but also causes an emerging disease in humans (Jalovecka et al., 2019). *Babesia* is a global pathogen that is more prevalent in certain regions such as Asia, Europe, and North America. However, as climate change brings with it higher temperatures and humidity, ticks and their reservoir hosts are anticipated to expand northward for survival and activity (Gray and Ogden, 2021). The disease is known as babesiosis, commonly characterized by fever and hemolytic anemia, but chronic infections can be asymptomatic (Almazán et al., 2022). The fatality rate ranges from 1% among all cases to 3% among hospitalized cases, and as high as 20% in immunocompromised patients (Krause, 2019).

Currently, the most common drugs for the treatment of human babesiosis include a combination of atovaquone (ATO) plus azithromycin (AZI) or clindamycin (CLN) plus quinine (QUI) (Krause et al., 2021). Still, these recommended treatments often result in various problems. For instance, multiple mutations in the *B. microti* cytochrome b, which is targeted by ATO, were identified in patients with relapsing babesiosis (Holbrook et al., 2023; Krause et al., 2024; Lemieux et al., 2016; Marcos et al., 2022; Rogers et al., 2023; Rosenblatt et al., 2021; Simon et al., 2017). The combination of CLN and QUI is the last resort for patients with severe symptoms (Kletsova et al., 2017). Despite its efficacy, this combination can elicit adverse drug reactions (Vannier and Krause, 2012). The 8-aminoquinoline analog tafenoquine (TQ) was found to be effective in curing immunocompromised patients experiencing relapsing babesiosis caused by *B. microti* (Rogers et al., 2023). However, the efficacy of TQ treatment may vary between individuals and cases and its contraindication in patients with glucose-6-phosphate dehydrogenase (G6PD) deficiency limits its clinical use (Chu and Freedman, 2019). Due to the aforementioned issues, it is undoubtedly urgent to search for compounds that treat infections caused by *Babesia* spp. while simultaneously minimizing the detrimental side effects of antibabesial drugs.

Spiroindolone cipargamin (CIP), a promising antimalarial, has been found to effectively suppress the growth of all strains of *Plasmodium falciparum* and *P. vivax* with potency in the low nanomolar ranges (Rosling et al., 2018; Rottmann et al., 2010). The assessment of the drug indicated that CIP taken orally had good absorption, a long half-life, and exceptional bioavailability (Schmitt et al., 2022). Following oral CIP treatment (30 mg daily for three days) in adults with simple *P. falciparum* or *P. vivax* malaria, parasitemia was rapidly cleared in a phase II trial (Schmitt et al., 2022). Currently, a clinical trial is being conducted for the intravenous administration of CIP as a treatment for severe malaria patients (ClinicalTrials, 2024). CIP was also evaluated for treating toxoplasmosis as a second-line medicine in cases where there are intolerable toxicity issues or allergies to the currently used treatments. Mice infected with *T. gondii* that were treated with CIP on the day of infection and the following day had 90% fewer parasites five days post-infection (Zhou et al., 2014).

*Pf*ATP4, a P-type ATPase in *P. falciparum*, functions as a Na^+/H^+ transporter critical for maintaining ionic balance (Spillman et al., 2013). Mutations in *Pf*ATP4 confer resistance to CIP, which disrupts Na^+ homeostasis, leading to increased cytosolic Na^+ concentration and various physiological changes, such as cytosolic alkalinization, osmotic swelling, etc. (Mohring et al., 2022). These mutations reduce the Na^+-dysregulating effects of CIP and the resting Na^+ levels. While *Pf*ATP4 is

essential for *P. falciparum* survival, its homolog in *T. gondii* (*Tg*ATP4) is less critical, as *T. gondii* experiences brief, high Na^+ exposure and can survive without *Tg*ATP4 expression (Lehane et al., 2019).

Due to its excellent efficacy against other apicomplexan parasites, including *Plasmodium* spp., and its ability to target parasite ATP4—a conserved protein essential for ion homeostasis in apicomplexan organisms—we hypothesize that CIP could also effectively inhibit *Babesia* spp., a related apicomplexan parasite. Therefore, the objectives of this study were to determine whether CIP could inhibit the growth of *Babesia* spp., namely *B. bovis* and *B. gibsoni in vitro* and *B. microti* and *B. rodhaini in vivo*, and identify the inhibitory mechanisms of CIP on *Babesia* parasites.

Results

Inhibitory efficacy of CIP on *B. bovis* and *B. gibsoni in vitro*

In vitro efficacy of CIP against *B. bovis* and *B. gibsoni* showed a steep growth inhibition curve with half inhibitory concentration (IC_{50}) values of 20.2 ± 1.4 nM (**Figure 1A**) and 69.4 ± 2.2 nM (**Figure 1B**), respectively. The 50% cytotoxic concentration (CC_{50}) value of CIP on Madin-Darby canine kidney (MDCK) cells and human foreskin fibroblasts (HFF) were 38.7 ± 2.0 μM and 70.8 ± 4.9 μM (**Figure supplement 1**), respectively. Based on these values, the predicted selectivity indices (SIs), which reflect the drug's safety and specificity, were calculated to be greater than 500. Furthermore, at a concentration of 100 μM, CIP exhibited a low erythrocyte hemolysis rate of 0.11 ± 0.03 % (data not shown).

CIP effect on B. microti and B. rodhaini infections in vivo

Concurrently, CIP showed effective inhibition on *B. microti* and *B. rodhaini in vivo*. The parasitemia of *B. microti*-infected BALB/c mice increased dramatically in the vehicle-treated control group and peaked at 10 days postinfection (DPI) (38.55 ± 4.32%) (**Figure 1C**). On the other hand, seven days of treatment with CIP (20 mg/kg) or atovaquone (ATO) plus azithromycin (AZI) administered orally resulted in a significantly lower peak parasitemia, 1.06 ± 0.20% and 1.61 ± 0.20%, respectively (**Figure 1C**). Hematocrit (HCT) variations were tracked every 4 days as an indicator of anemia in *B. microti*-infected mice. The vehicle-treated group showed a drop in HCT levels at 12 DPI and 16 DPI ($P < 0.01$) (**Figure 1D**). No significant reduction in HCT levels was observed in the CIP-treated group or the ATO plus AZI-treated group (**Figure 1D**). This indicates that the administration of CIP could control *B. microti* infection and prevent anemia from developing in *B. microti*-infected mice. BALB/c mice infected with *B. rodhaini* treated with sesame oil or ATO plus AZI showed high parasitemia, 90.73 ± 1.97%, and 86.23 ± 3.06%, respectively (**Figure 1E**), and all mice died within 8 DPI (**Figure 1F**). CIP treatment in *B. rodhaini*-infected mice precluded the emergence of parasitemia for the following eight days (**Figure 1E**), which led to 66.67% of mice surviving the challenge infection (**Figure 1F**). At 12 DPI, parasites had recurred in all CIP-treated *B. rodhaini*-infected mice (10.32 ± 15.51%), which were eventually cleared as indicated by undetectable parasites at 18 DPI (**Figure 1E**).

Identification of *B. gibsoni* ATP4 mutation in CIP-resistant strains

After being exposed to CIP at increasing concentrations up to 10 times the IC_{50}, the resistant parasites in two of the culture wells were able to regrow. We sequenced the *B. gibsoni* ATP4 gene from the wild-type and two resistant strains. The wild-type strain has a C at nucleotide 2,761, which translates to leucine (**Figure 2A**). In one resistant strain, a single nucleotide variant (SNV) in *Bg*ATP4 with a substitution at position 2,761 (from C to G) was found – a nonsynonymous coding change from leucine to valine (L921V) (**Figure 2B**). In another resistant strain, the mutation occurred in the same position. However, the nucleotide substitution was from C to A, and the

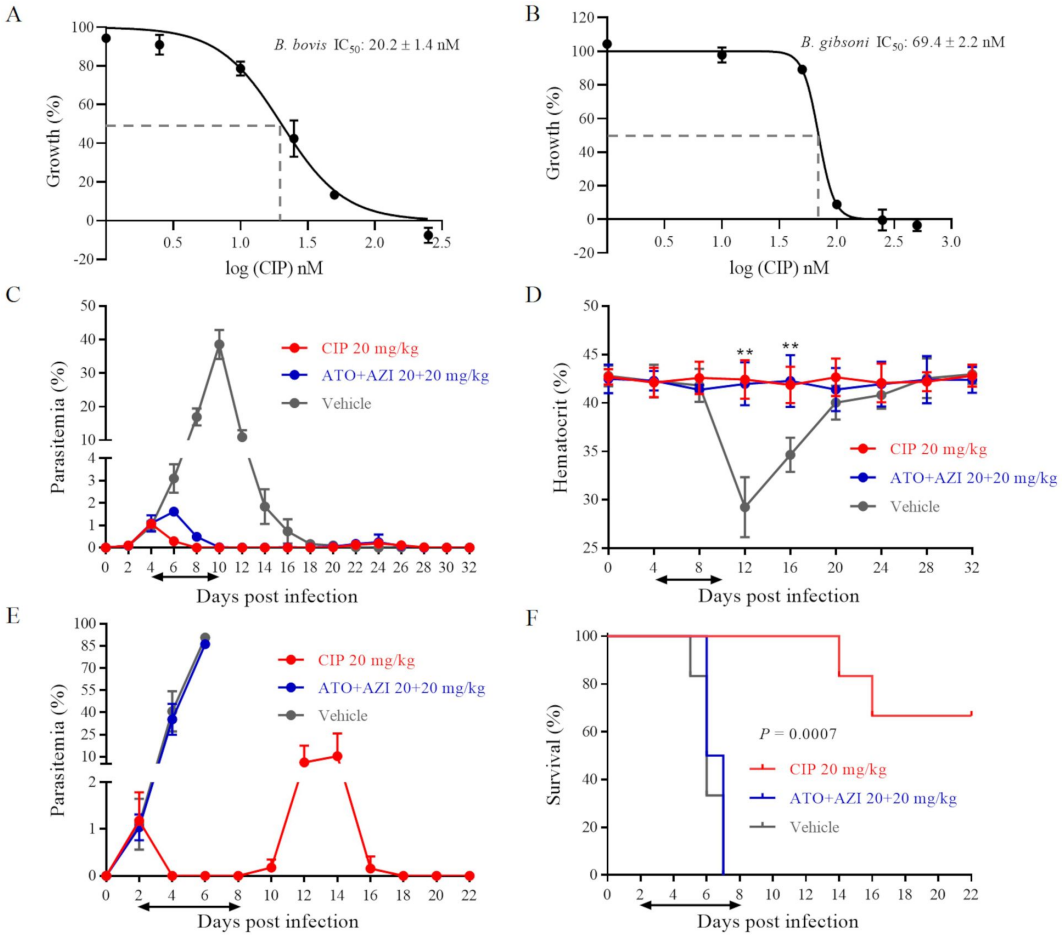

Figure 1.

CIP demonstrates potent inhibition on *Babesia* spp..

(A) and **(B)** Dose-dependent growth curve of CIP on *B. bovis* and *B. gibsoni in vitro*. Each value represents the mean ± standard deviation (SD) of three independent experiments carried out in triplicate. IC_{50}: the half maximal inhibitory concentration. **(C)** Inhibitory effects of CIP and atovaquone (ATO) plus azithromycin (AZI) on the proliferation of *B. microti* in BALB/c mice. **(D)** Hematocrit (HCT) values in mice treated with CIP or ATO plus AZI compared with vehicle-treated mice. **(E)** Inhibitory effects of CIP and ATO plus AZI on the proliferation of *B. rodhaini* in BALB/c mice. **(F)** Survival rates of CIP-treated, ATO plus AZI-treated, and vehicle-treated mice. The treatment time is shown by two-way arrows, and significant differences ($P < 0.01$) between the drug-treated groups and the vehicle-treated control group are indicated by asterisks. The data from one of six individual experiments are expressed as means ± SD. *, $P < 0.05$; **, $P < 0.01$.

coding changed from leucine to isoleucine (L921I) (**Figure 2C**). Next-generation sequencing (NGS) revealed that for *Bg*ATP4^{L921V}, 99.97% of 7,960 reads were G at nucleotide 2,761, and for *Bg*ATP4^{L921I}, 99.92% of 7,862 reads were A at nucleotide 2,761 (**Figure 2D**). *Bg*ATP4^{L921V} and *Bg*ATP4^{L921I} lines were tested for their susceptibility to CIP, and had IC_{50} values of 421.0 ± 15.9 nM and 887.9 ± 62.0 nM, respectively (**Figure 2E**). These findings demonstrate a 6.1- and 12.8-fold reduction in CIP sensitivity of the resistant parasite lines *Bg*ATP4^{L921V} and *Bg*ATP4^{L921I}.

The effect of CIP on *Bg*ATP4^{WT}, *Bg*ATP4^{L921V} and *Bg*ATP4^{L921I} function

Microscopic observation of thin blood smears was performed to determine the morphological changes of *B. gibsoni* exposed to CIP. The CIP-treated parasites became swollen after incubation with the drug for 72 h (**Figure 3A**). For both the treatment and control groups, one hundred parasites were measured. The mean size of treated parasites was notably bigger than the parasites in the untreated group ($P < 0.0001$) (**Figure 3B**). Significant vacuolization was observed in the cytoplasm of parasites in the CIP-treated group, as revealed by transmission electron microscopy (TEM). Despite this, the nuclear membrane structure and parasitic membranes remained intact until the parasites were completely destroyed (**Figure 3C**). The addition of the ATP4 inhibitor CIP resulted in a time-dependent increase in the concentrations of $[Na^+]_i$ in wild-type *B. gibsoni*, with improved signal-to-noise ratios at the higher drug concentration of 20 nM (**Figure 3D**). We observed that the Na^+ concentrations in both *Bg*ATP4^{L921V} and *Bg*ATP4^{L921I} lines were lower when compared with those of the control *Bg*ATP4^{WT} line after being exposed to 20 nM CIP for 20 min, with a significantly lower Na^+ concentration in *Bg*ATP4^{L921I} ($P = 0.0087$) (**Figure 3F**). We also demonstrated here that the addition of CIP in wild-type *B. gibsoni* caused an increase in the cytosolic pH (**Figure 3E**). Specifically, 4 min after the drug was added, the average pH of 20 nM CIP group reached as high as 7.278, while the 1 nM CIP group reached 7.089 and the untreated group reached 7.062 (**Figure 3E**). The pH values of the 20 nM CIP group were consistently higher than those of the other two groups, although declining with time (**Figure 3E**). In resistant lines, a 20-min exposure to 20 nM CIP caused small changes in the pH values compared to the wild-type line, with the *Bg*ATP4^{L921I} line (7.048 ± 0.042) having a notably lower pH value ($P = 0.0229$) (**Figure 3G**).

Sensitivity of *Bg*ATP4-associated ATPase activity to CIP in *Bg*ATP4^{WT}, *Bg*ATP4^{L921V} and *Bg*ATP4^{L921I}

The *Bg*ATP4-associated ATPase activity in erythrocytes infected with *Bg*ATP4^{WT} (6.31 ± 1.20 nmol Pi/mg protein/min), measured in the presence of 150 mM Na^+, was higher than that observed in *Bg*ATP4^{L921V} (5.11 ± 0.50 nmol Pi/mg protein/min) and *Bg*ATP4^{L921I} (4.58 ± 0.53 nmol Pi/mg protein/min) ($P = 0.04$) (**Figure 3H**).

We further investigated the concentration-dependent inhibition of *Bg*ATP4-associated ATPase activity by CIP in wild-type and mutant parasites. In membranes prepared from *B.gibsoni*, CIP inhibited *Bg*ATP4-associated ATPase activity with IC_{50} values of 111.4 ± 31.8 nM for *Bg*ATP4^{WT}, 149.8 ± 21.7 nM for *Bg*ATP4^{L921V}, and 269.5 ± 29.8 nM for *Bg*ATP4^{L921I}. The potency of CIP in inhibiting *Bg*ATP4-associated ATPase activity was reduced by 1.3-fold and 2.4-fold in membranes prepared from *Bg*ATP4^{L921V} and *Bg*ATP4^{L921I}, respectively, compared to *Bg*ATP4^{WT} (**Figure 3I**).

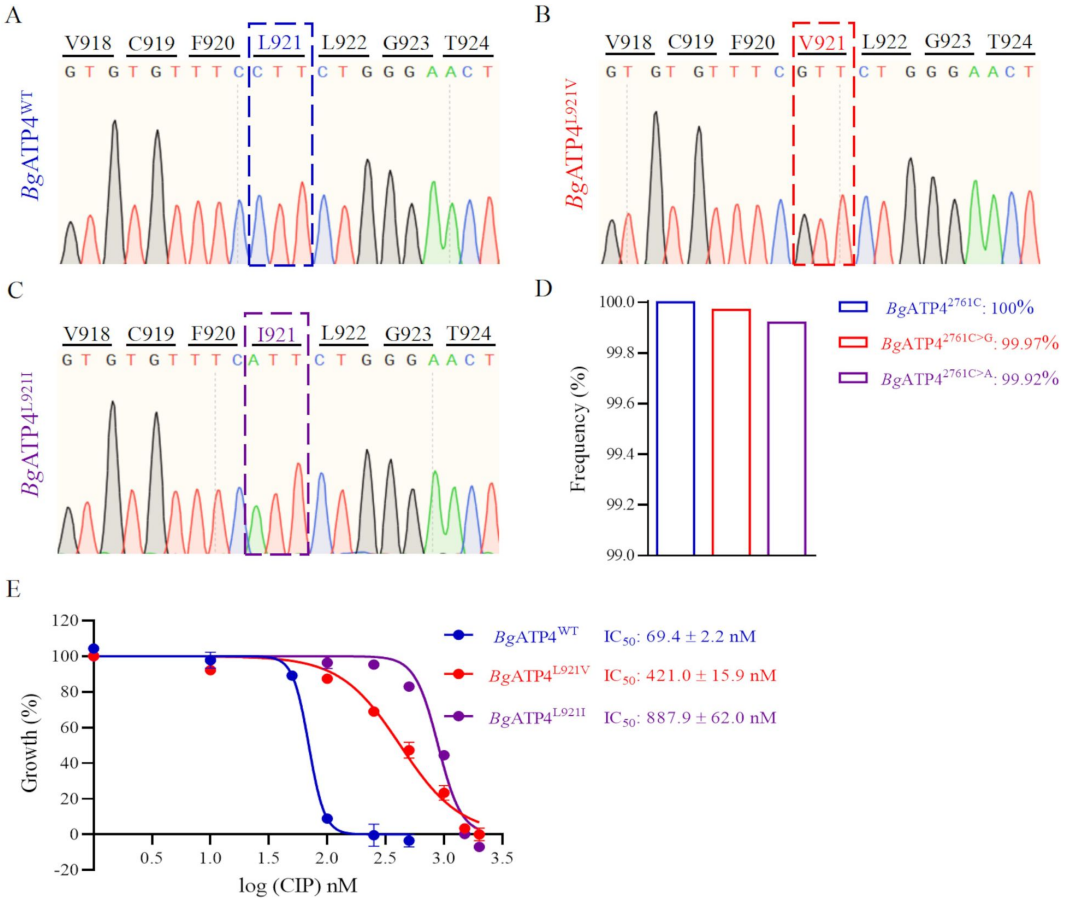

Figure 2.

Mutations in *Bg*ATP4 mediate CIP resistance.

(A-C) Representative sequencing chromatogram of wild-type and resistant parasites from CIP-treated *B. gibsoni*. The resistant parasite genomic DNA is extracted from blood samples after a 60 day-treatment. The *Bg*ATP4 gene was amplified and sequenced using the DNA. (**D**) Genes of high-frequency sequence variants detected by NGS. (**E**) Dose-dependent growth curve of *Bg*ATP4^{WT}, *Bg*ATP4^{L921V}, and *Bg*ATP4^{L921I} *in vitro*. Each value represents the mean ± standard deviation (SD) of three independent experiments carried out in triplicate.

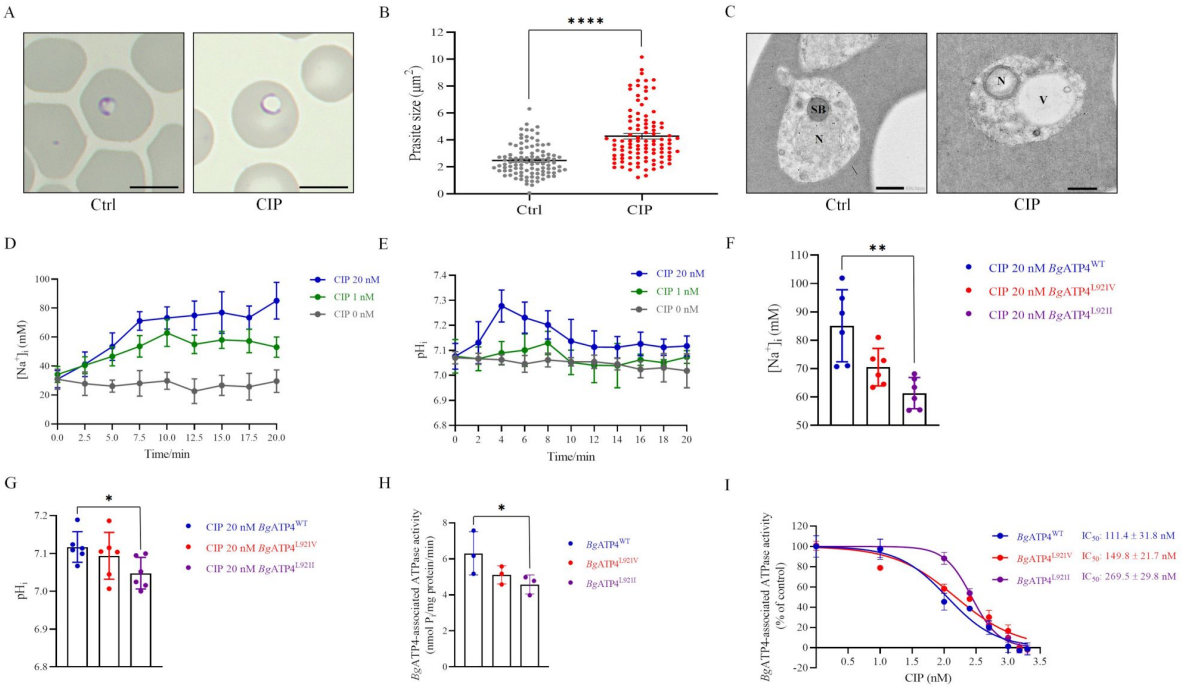

Figure 3.

Mechanistic basis for resistance to CIP conferred by the L921V and L921I mutations in *Bg*ATP4.

(A) Untreated and CIP-treated parasite morphology after incubation for 72 h. Scale bar: 5 μm. (**B)** Sizes of 100 parasites in two groups measured with ImageJ software in panels A. Statistically significant differences between the means of variables determined by t-test. ****, $P < 0.0001$. (**C)** TEM of untreated and CIP-treated parasite. N, Nucleus; SB, spherical body; V, vacuole. Scale bar: 500 nm. (**D)** $[Na^+]_i$ concentrations after addition of CIP in *Bg*ATP4^{WT} line. Representative traces from the experiment that highlight the impact of adding 20 nM CIP (blue), 1 nM CIP (green), or 0 nM CIP (grey) on the concentration $[Na^+]_i$ of the *Bg*ATP4^{WT} line. (**E)** Alkalinization of pH_i in *Bg*ATP4^{WT} line upon addition of the ATP4 inhibitor. (**F)** Addition of 20 nM CIP to the wild-type and resistant parasite lines results in different $[Na^+]_i$ concentrations. (**G)** Addition of 20 nM CIP to the wild-type and resistant parasite lines results in different pH_i concentrations. Experiments were performed in technical duplicates for at least three biological repeats. **(H)** Data acquired in the low Na^+ condition (containing only the 2 mM Na^+ introduced upon addition of 1 mM Na_2ATP) was subtracted from data obtained in the high Na^+ condition to determine the ATPase activity related to the *Bg*ATP4 proteins. The results are presented as the average of data from three independent tests. (**I)** Dose-dependent *Bg*ATP4-associated ATPase activity curve of *Bg*ATP4^{WT}, *Bg*ATP4^{L921V}, and *Bg*ATP4^{L921I} *in vitro*. ATPase activity was determined at pH 7.2 in the presence of 150 mM Na^+ and 1mM Na_2ATP. Each value represents the mean ± standard deviation (SD) of three independent experiments carried out in triplicate. *, $P < 0.05$; **, $P < 0.01$.

Multiple sequence alignment of *Babesia* ATP4 and molecular docking

The whole amino acid sequence of *B. gibsoni* ATP4 (GenBank: KAK1443404.1) shared identity values of 29.75%, 49.40%, 49.67%, 62.21%, and 52.47% with *Homo sapiens* ATP4 (GenBank: NM_000704.3), *P. falciparum* ATP4 (GenBank: PF3D7_1211900), *T. gondii* ATP4 (GenBank: XP_018635122.1), *B. bovis* ATP4 (PiroplasmaDB: BBOV_IV010020), and *B. microti* ATP4 (GenBank: BMR1_03g01005), respectively (**Figure supplement 2**).

The pLDDT (predicted Local Distance Difference Test) value of *Bg*ATP4^{WT} prediction was 80.7 using Colab-fold. Multiple potential binding sites for CIP were revealed by blind docking throughout the whole protein surface (**Figure supplement 3**). CIP binds in close proximity to L921, as demonstrated by focused docking on this area (**Figure 4A**). The contribution of each residue to the predicted binding affinity in either mutant structure was reduced; the precise values of *Bg*ATP4^{WT} (**Figure 4B**), *Bg*ATP4^{L921V} (**Figure 4C**), and *Bg*ATP4^{L921I} (**Figure 4D**) were -6.43, -6.40 and -6.26 kcal/mol, respectively. The interactions of CIP from each docking simulation are shown in **Table supplement 3**.

Cross-resistance of *Bg*ATP4^{L921V} and *Bg*ATP4^{L921I} mutants to ATO and TQ

The *Bg*ATP4^{WT}, *Bg*ATP4^{L921V}, and *Bg*ATP4^{L921I} lines were tested for their susceptibility to ATO and TQ. The IC_{50} values for these lines were 380.1 ± 3.1 nM, 412.9 ± 5.4 nM, and 360.3 ± 7.9 nM, respectively, for ATO (**Figure 5A**), and 39.5 ± 0.4 μM, 29.9 ± 1.4 μM, and 39.3 ± 0.3 μM, respectively, for TQ (**Figure 5B**). The IC_{50} values for both ATO and TQ in the resistant strains showed only slight changes compared to the wild-type strain, with less than a onefold difference. This minimal variation suggests that the resistant strain has a mild alteration in susceptibility to ATO and TQ, but not enough to indicate strong resistance or significant cross-resistance.

Combination treatment of CIP plus TQ in SCID mice with *B. microti* infection

The parasitemia of *B. microti*-infected SCID mice in the vehicle group increased dramatically, peaking at 10 DPI (77.03 ± 2.45%) (**Figure 5C**). Although the trend showed a subsequent decline, the parasitemia remained around 50% until the mice were euthanized at 90 DPI. Treatment with CIP (20 mg/kg) initially reduced parasitemia to undetectable by 18 DPI. However, a relapse occurred, with parasitemia increasing rapidly and stabilizing at levels comparable to the vehicle group during the subsequent observation period. Notably, no mutations were detected in the relapsed *B. microti* parasites from SCID mice (data not shown). In contrast, parasitemia was completely cleared in the TQ and CIP plus TQ groups by 8 DPI and 6 DPI, respectively, with no parasites observed under the microscope thereafter. Absolute qPCR analysis at 90 DPI detected parasite DNA in all groups except the CIP plus TQ group (**Figure 5D**).

Discussion

The repositioning of antimalarial drugs is critical in developing novel strategies for treating babesiosis. CIP is a novel compound that inhibits *Plasmodium* development by targeting ATP4 and has been extensively tested in Phase 1 and Phase 2 clinical trials (Qiu et al., 2022). Since ATP4 is conserved across apicomplexans, including *Babesia* species, our study aimed to repurpose the

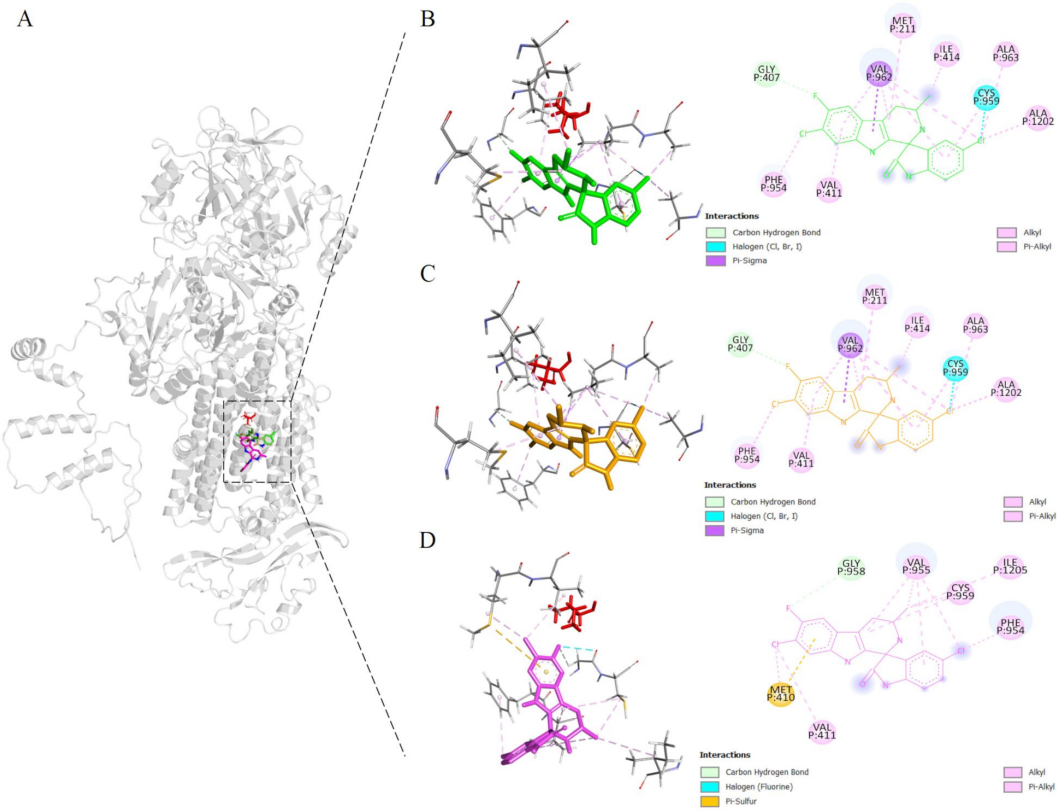

Figure 4.

Binding sites proximal to *Bg*ATP4 residue 921 predicted by molecular docking.

(A) The lowest energy poses for CIP were located in reference to the whole protein structure, docking against the WT (green), L921V (yellow), and L921I (pink) mutant *Bg*ATP4. The side chain of L921 is also shown in a red stick at its position. (**B**-**D)** The zoomed views of the binding locations of CIP.

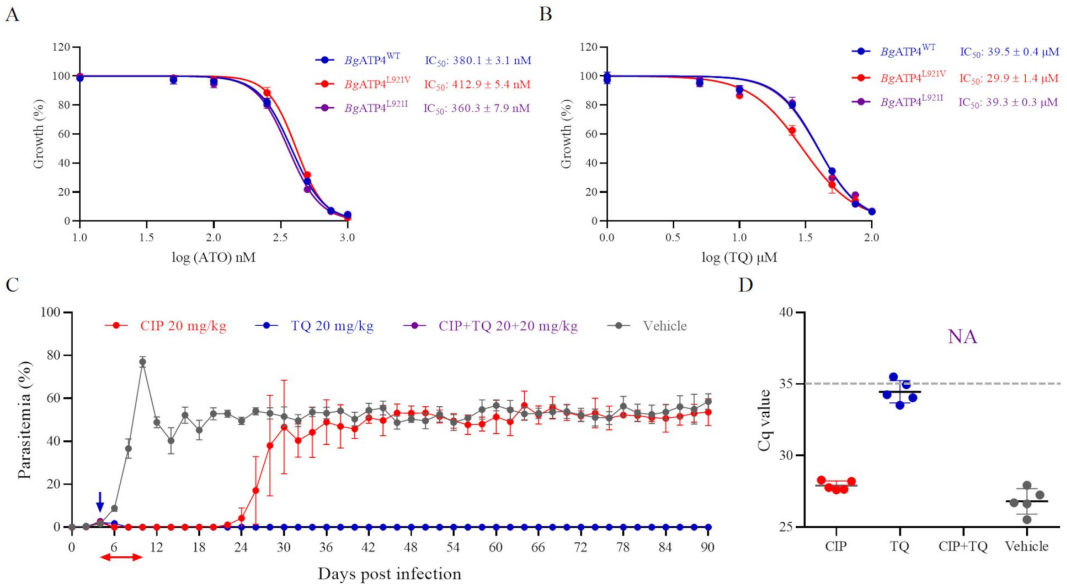

Figure 5.

Cross-resistance between ATO and TQ in resistant parasites and combination therapy based on CIP plus TQ.

(A) Dose-dependent growth curve of *Bg*ATP4^{WT}, *Bg*ATP4^{L921V}, and *Bg*ATP4^{L921I} by ATO treatment *in vitro*. **(B)** Dose-dependent growth curve of *Bg*ATP4^{WT}, *Bg*ATP4^{L921V}, and *Bg*ATP4^{L921I} by TQ treatment *in vitro.* Each value represents the mean ± standard deviation (SD) of three independent experiments carried out in triplicate. **(C)** Inhibitory effects of CIP plus TQ on the proliferation of *B. microti* in SCID mice. The data are presented as the means from one of five independent experiments. **(D)** Parasite DNA was detected by qPCR on genomic DNA extracted from blood collected from untreated and treated SCID mice infected with *B. microti* at 90 DPI. A dotted grey line across the graph represents the average cut-off Cq value. Cut-off Cq ≤ 35 was considered as positive, while Cq > 35 or no amplification was considered as negative. Each sample was analyzed in duplicate, and two independent experiments were conducted. NA indicates no amplification.

antimalarial CIP by assessing its efficacy on *Babesia* species (Lehane et al., 2019). The IC_{50} values of CIP against *B. bovis* and *B. gibsoni in vitro* were lower than the previously reported IC_{50} value of TQ (Carvalho et al., 2020; Ji et al., 2022b) and ATO against *B. gibsoni* (Matsuu et al., 2004). The present investigation also demonstrated that the inhibitory effects of CIP on *B. microti*-infected BALB/c mice were comparable to that of ATO plus AZI, the combination recommended by the CDC in the United States. CIP was also proven to protect mice from the deadly *B. rodhaini* infection, with survival up to 67%, as recorded in the current trial. These results suggest that CIP may be a potential chemotherapy candidate for babesiosis.

In a previous study, the *P. falciparum* Dd2 strain that acquired resistance to CIP carried the G358S mutation in the *Pf*ATP4 protein, a *P. falciparum* P-type Na^+ ATPase (Qiu et al., 2022). The vital protein ATP4 is found in the parasite plasma membrane and is specific to the subclass of apicomplexan parasites (Mohring et al., 2022). To date, *in vitro* evolution experiments using CIP have produced at least 18 parasite lines with various *Pf*ATP4 mutations (Lee and Fidock, 2016; Rottmann et al., 2010). In another study involving *T. gondii*, a cell line that carried the mutation G419S in the *Tg*ATP4 gene was 34 times less susceptible to CIP than that of $TgATP4^{WT}$ (Qiu et al., 2022). It follows that there is a significant chance that the resistant *Babesia* parasites will also emerge from CIP exposure. In this study, we successfully produced two CIP-resistant strains using six independent selections. The newly discovered L921V and L921I mutations in *Bg*ATP4 decreased the CIP sensitivity by 6.1 and 12.8 times, respectively. We provided compelling evidence that natural variety mutations L921V and L921I in *Bg*ATP4 significantly affected the protein's susceptibility to CIP inhibition, albeit the mutational sites were different from those of *P. falciparum* and *T. gondii*. Based on our observation, the growth and generation rates of the mutant strains are comparable to those of the wild-type strain.

Although ATP4 was initially recognized as a Ca^{2+} transporter (Krishna et al., 2001), current evidence suggests that ATP4 functions as an ATPase for exporting Na^+ while importing H^+ (Mohring et al., 2022), as well as causing a variety of other physiological perturbations including an increase in the volume of parasites and infected erythrocytes, due to the osmotic impact of the $[Na^+]_{cyt}$ increase (Dennis et al., 2018), a decline in cholesterol extrusion from the parasite plasma membrane as a result of the increase in $[Na^+]_{cyt}$ (Das et al., 2016), and an intensified rigidity of erythrocytes infected with ring-stage parasites (Zhang et al., 2016). In this study, the CIP-exposed wild-type *B. gibsoni* became swollen, which was identical to a prior study on *P. falciparum* (Dennis et al., 2018). Interestingly, TEM analysis of parasites incubated with CIP revealed ultrastructural alterations characterized by significant vacuole formation in the cytoplasm, a hallmark of stress or early stages of cell death. These changes were similar to those observed in *B. bovis* treated with clotrimazole and ketoconazole, which ultimately led to growth inhibition or parasite death (Bork et al., 2003). Despite the vacuolization, the structural integrity of the nucleus and membranes was maintained, suggesting a gradual process where vacuolization precedes the complete destruction of the parasite. One explanation is the swelling of the isolated parasites, which can be ascribed to the osmotic consequences of Na^+ uptake and is contingent upon the presence of Na^+ in the external environment.

The output of Na^+ and input of H^+ diminished upon CIP-induced inhibition of *Pf*ATP4, and the continued outflow of H^+ via V-type H^+-ATPase led to an alkalinization that ultimately killed the parasites (Spillman et al., 2013). Our capacity to measure a time-dependent increase in the concentration of $[Na^+]_i$ and pH value for wild-type *B. gibsoni* facilitated us to gain insight into the basic mechanisms of CIP on $BgATP4^{WT}$ function. Furthermore, our results validate that internal alkalinization was the main factor in *Babesia* death and support our hypothesis that the swollen isolated parasites were produced by Na^+ absorption. To explore further how mutations in *Bg*ATP4 are associated with the upregulation of the parasite's $[Na^+]_i$ and $[H^+]_i$, we tested two *Bg*ATP4-mutant lines that were chosen previously with *Bg*ATP4 inhibitors ($BgATP4^{L921V}$ and $BgATP4^{L921I}$). Due to the presence of L921V and L921I mutations in drug-resistant strains of *Bg*ATP4, the concentration of Na^+ did not increase as much as it would have in the wild-type strain following

the addition of 20 nM CIP for 20 min. As intraerythrocytic alkalinization rises, the same outcome happens. From these results, we deduced how natural mutations in *Bg*ATP4 may affect ATP4 inhibitor susceptibility by dysregulating H^+ and Na^+ balance, which helped parasites survive in a relatively high concentration of CIP. An illustration of the putative processes for regulating Na^+ and H^+ in erythrocytes infected with the *Babesia* parasite is presented in **Figure supplement 4**.

In a previous study's isolated membrane assay, CIP was found to be more effective at inhibiting parasite development than *Pf*ATP4-associated ATPase activity and reduced sensitivity of *Pf*ATP4-associated ATPase activity to the medication was associated with a decrease in parasite susceptibility to CIP (Rosling et al., 2018). In our study, the higher resistance to CIP-mediated inhibition of parasite proliferation observed in *Bg*ATP4^{L921I} compared to *Bg*ATP4^{L921V} correlated with a higher resistance of *Bg*ATP4-associated ATPase activity to the drug. These findings provide additional evidence that the ATPase activity measured in this study corresponds to the activity of the *Bg*ATP4 protein.

According to studies using the *Pf*ATP4 model for molecular docking, the G358S mutation results in a steric clash that lowers CIP's binding affinity (Qiu et al., 2022). The results from the current study were similar to the *Pf*ATP4 model. The molecular docking was constructed using a ColabFold model of wild-type *Bg*ATP4, which predicted the binding mode and affinity between ATP4 protein and the ligand to provide a possible mechanistic explanation. It suggested that the L921V mutation caused changes at the atomic level, whereas the L921I mutation created a steric clash that reduced the binding affinity of CIP. The predicted affinity score of the L921I mutation was lower than that of the L921V mutation. Thus, it is possible that CIP had a weaker binding to *Bg*ATP4^{L921I} than to *Bg*ATP4^{L921V}. These findings are consistent with the results obtained from measuring the IC_{50} of the drug against parasites with the L921V and L921I mutations.

While CIP shows promise as an antibabesial agent, the emergence of resistance emphasizes the importance of rational drug use and the development of combination therapies. Our results demonstrate that CIP did not exhibit cross-resistance with ATO or TQ, as IC_{50} values for ATO and TQ in resistant strains showed minimal changes (<1-fold) compared to the wild-type strain. This observation suggests that CIP could be effectively combined with other anti-babesial drugs to reduce the risk of resistance development. Previous studies have also reported that a single dose of TQ may not be sufficient to prevent parasite relapse in immunocompromised hosts, recommending either repeated TQ administration or combination therapy with other antibabesial agents to address this issue (Liu et al., 2024). Supporting this approach, our study demonstrates that the combination of CIP plus TQ effectively cleared *B. microti* infections in SCID mice, with no detectable parasitemia or DNA observed at 90 DPI, indicating complete parasite elimination.

This preclinical finding underscores the potential of the CIP plus TQ combination as a viable treatment strategy for babesiosis, especially in cases where monotherapy is ineffective. Further studies are needed to fully explore the pharmacokinetics, long-term efficacy, and potential side effects of such combinations in clinical settings, ultimately facilitating optimized therapeutic strategies.

In summary, our findings provide a comprehensive understanding of CIP's efficacy, mechanism of resistance, and identifying strategies to enhance its therapeutic potential. The combination of CIP with drugs like TQ offers a promising approach to combat babesiosis and mitigate the development of resistance.

Materials and methods

Parasite culture

The parasites *B. gibsoni* Oita strain and *B. bovis* Texas strain were *in vitro* cultured in 24-well plates and maintained in an atmosphere of 5% CO_2 and 5% O_2 at 37 °C (Liu et al., 2018). For the *in vivo* studies, *B. microti* Peabody mjr strain-(ATCC PRA-99^{TM}) and *B. rodhaini* Australia strain-infected RBCs (iRBCs), which were collected and diluted with phosphate-buffered saline (PBS) when the parasitemia levels in the donor mice reached ~20% and 50%, respectively, and were intraperitoneally injected into BALB/c mice. Each BALB/c mouse was infected with 1.0×10^7 *B. microti* or *B. rodhaini* iRBCs for the *in vivo* trials (Ji et al., 2022a).

In vitro cytotoxicity of CIP and hemolysis rate in canine erythrocytes

Cultures of Madin-Darby canine kidney (MDCK) cells and human foreskin fibroblasts (HFF) were maintained at 37 °C under an atmosphere of 5% CO_2 and 5% O_2 and the cytotoxic effect of CIP (MedChem Express, Tokyo, Japan) was assessed using a cell viability assay by CCK-8 (Dojindo, Japan) as described previously (Li et al., 2023). The selectivity index is calculated as the ratio between the half maximal inhibitory concentration (IC_{50}) and the 50% cytotoxic concentration (CC_{50}) values.

Canine erythrocytes were collected from healthy beagle dogs raised in NRCPD and stocked in Vega y Martinez (VYM) phosphate-buffered saline solution at 4 °C (Vega et al., 1985). A canine erythrocyte hemolysis assay was performed at concentrations of 0.1, 1, 5, 10, 25, 50, and 100 μM as previously described (Ariefta et al., 2022).

Evaluation of the efficacy of CIP against *Babesia* parasites *in vitro*

The efficacy of CIP against *B. gibsoni* and *B. bovis* was determined using a fluorescence assay, as previously described (Guswanto et al., 2014). The IC_{50} values were determined from the fluorescence values and by non-linear regression analysis (curve fit) in GraphPad Prism 9 (GraphPad Software Inc., USA).

Chemotherapeutic effects of CIP against *Babesia* infections *in vivo*

CIP was evaluated on *B. microti*- and *B. rodhaini*-infected mice, as previously described (Ndayisaba et al., 2021; Tuvshintulga et al., 2022). When *B. microti*- and *B. rodhaini*-infected mice had a 1% average parasitemia at 4 and 2 days postinfection (DPI), respectively, the drug treatments were administered and continued for seven days. Three groups of *B. microti*-infected mice were administered different treatments. The CIP group (n = 6) and the ATO plus AZI group (n = 6) were orally treated with 20 mg/kg CIP and 20 mg/kg ATO plus 20 mg/kg AZI (Sigma, Tokyo, Japan), respectively. All drugs were prepared in sesame oil. The infected mice of the vehicle group (n = 6) orally received 0.2 mL of sesame oil as the control. Eighteen mice infected with *B. rodhaini* were likewise placed into three groups for treatment, and they received the same treatments as the mice infected with *B. microti*. A light microscope (Nikon, Japan) and a hematology analyzer (Celltac α MEK-6450, Nihon Kohden Corporation, Tokyo, Japan) were used to assess the parasitemia and hematocrit levels every two and four days, respectively.

Selection of CIP-resistant *B. gibsoni in vitro*

Selections were initiated by exposing six independent flasks, each containing 10 μL (5×10^6) *B. gibsoni* iRBCs mixed with 40 μL (4×10^8) RBCs into a 450 μL culture medium, which contained increasing concentrations of CIP: 5, 10, 20, 30 to 694 nM ($10\times IC_{50}$). The medium containing CIP was replaced daily until parasites treated with $10\times IC_{50}$ CIP reached multiplication rates that were

approximately comparable to those of the untreated controls (Hwang et al., 2010). Then, to evaluate the decreased sensitivity to CIP, IC_{50} values of resistant strains were determined by nonlinear regression using the GraphPad Prism software.

Detection of *B. gibsoni* ATP4 gene mutations

The genomic DNA of the mutant parasites was extracted and sequenced (Ji et al., 2022a). The primer sets used for sequencing are listed in **Table supplement 1**. The single nucleotide variants were identified by pairwise alignment to the *Bg*ATP4^{WT} sequence (GenBank: JAVEPI010000002.1). Next-generation sequencing (NGS) was performed to detect the ratio of wild-type to mutant parasites by using the Illumina NovaSeq6000 sequencing platform (Jeon et al., 2021).

Morphological changes in CIP-treated *in vitro* cultured *B. gibsoni*

A microscopy assay was used to detect the morphological changes of wild-type *B. gibsoni* after exposure to 50 nM CIP for three consecutive days (Liu et al., 2021; Tayebwa et al., 2018). At 4 days post-treatment, ImageJ software was used to measure the sizes of 100 randomly selected parasites in the CIP-treated group and the control group on Giemsa-stained blood smears. After treating the parasites as described above, iRBCs were fixed in GA fixation buffer (2% glutaraldehyde in 0.1 M sodium cacodylate buffer containing 1 mM $CaCl_2$ and 1 mM $MgCl_2$), then stored in rinse buffer (0.1 M sodium cacodylate buffer containing 1 mM $CaCl_2$ and 1 mM $MgCl_2$) at 4 °C for transmission electron microscopy (TEM) analysis (Hidayati et al., 2023).

Parasites $[Na^+]_i$ and pH_i measurements

For both $[Na^+]_i$ and pH_i measurements, the wild-type and mutant parasites were initially separated from erythrocytes by treatment with saponin (0.05% [wt/vol]) for 5 min (Saliba and Kirk, 1999). The Na^+-sensitive fluorescent dye SBFI (Thermo Fisher Scientific; product S1263) was used to quantify intracellular sodium ($[Na^+]_i$). Saponin-isolated parasites (at 1×10^8 parasites/mL) were loaded with SBFI (5 µM; in the presence of 0.02% w/v Pluronic F127) for 1 hr at room temperature (RT) (Spillman et al., 2013). Thereafter, SBFI-loaded parasites were resuspended in physiological saline (120 mM NaCl, 5 mM KCl, 25 mM HEPES, 20 mM D-glucose, and 1 mM $MgCl_2$ [pH 7.1]) at RT in the presence or absence of CIP. A 96-well microtiter plate was filled with around 200 µL of parasite suspension per well. The dye-loaded cells fluoresced at 515 nm after being stimulated at 340 and 380 nm. Parasites loaded with SBFI were suspended in calibration buffers containing $[Na^+]$ values ranging from 0 to 140 mM (pH 7.1) to establish calibration curves (Diarra et al., 2001).

The cytosolic pH of wild-type and mutant strains was measured using the pH-sensitive fluorescent dye BCECF [2',7'-bis-(2-carboxyethyl)-5-(and-6)-carboxyfluorescein] (Biotium; product 51011). The BCECF was added to saponin-isolated parasites by suspension (1×10^8 parasites/mL) and incubated for 20 minutes at 37 °C in RPMI-1640 culture medium (Gibco, USA) (Saliba and Kirk, 1999). Thereafter, the parasites loaded with dye were rinsed thrice (12,000 × g, 1 min) in RPMI-1640 culture medium, then resuspended in physiological saline (as previously mentioned) with or without various concentrations of CIP. A 96-well microtiter plate was filled with around 200 µL of parasite suspension per well. The dye-loaded cells fluoresced at 520 nm after being stimulated at 440 and 490 nm. A pH calibration was carried out for each experiment (Mohring et al., 2022).

Measurements of membrane ATPase activity

Membranes from isolated *B. gibsoni* were prepared by lysing the parasites in ice-cold deionized water containing 7 × Protease Inhibitor Cocktail Tablets (Roche, Germany). The membrane preparation was then washed three times with ice-cold deionized water, with protease inhibitors included in the first two washes (Qiu et al., 2022). Protein concentrations in the membrane

samples were determined using a Bradford assay. The production of inorganic phosphate (Pi) from ATP hydrolysis was measured using the Malachite Green Phosphate Assay (BioAssay Systems, USA). Membrane preparations were diluted in either a high Na^+ solution (final reaction conditions: 150 mM NaCl, 20 mM KCl, 2 mM $MgCl_2$, 50 mM Tris, pH 7.2) or a Na^+-free solution (final reaction conditions: 150 mM choline chloride, 20 mM KCl, 2 mM $MgCl_2$, 50 mM Tris, pH 7.2) to achieve a final protein concentration of 40 µg/mL. CIP was added at the concentrations specified in the respective figure legends. Reactions were conducted according to the manufacturer's protocol provided with the assay kit.

Multiple ATP4 sequence alignment and molecular docking

B. gibsoni ATP4 (GenBank: KAK1443404.1), *B. bovis* ATP4 (PiroplasmaDB: BBOV_IV010020), *B. microti* ATP4 (GenBank: BMR1_03g01005), *T. gondii* ATP4 (GenBank: XP_018635122.1), and *Homo sapiens* ATP4 (GenBank: NM_000704.3) sequences were obtained by a homology search using *P. falciparum* ATP4 (GenBank: PF3D7_1211900). Sequence alignment was analyzed using MUSCLE in Jalview v2.11.3.2 software and BLAST (*http://www.ncbi.nlm.nih.gov/BLAST/*).

AlphaFold was used to predict the structure of *Bg*ATP4^{WT} (Jumper et al., 2021). Using the GROMACS 2021 Molecular Dynamics package, the energy minimization was carried out following the model's generation (Lindahl et al., 2021). The mutations were produced by using Charmm-GUI PDB reader (Jo et al., 2014). PyMol (version 2.0 Schrödinger, LLC) was used to confirm the position of the mutation site (center: -20.367, 10.904, 9.435; size: 30×30×30) (Trott and Olson, 2010). The ligand molecules CIP was downloaded from PubChem (CID 44469321 (*https://pubchem.ncbi.nlm.nih.gov/compound/* 44469321). The ligand was used to dock with Gnina (Eberhardt et al., 2021). The affinity score and binding pose were chosen only from the highest CNN (convolutional neural network) score results from docking simulations. The models were visualized using the PyMOL Molecular Graphic System and Discovery Studio.

Cross-resistance to TQ and ATO in mutant parasites

The efficacy of TQ and ATO against *Bg*ATP4^{WT}, *Bg*ATP4^{L921V}, and *Bg*ATP4^{L921I} was evaluated using a fluorescence assay, as described above. The IC_{50} values were calculated from the fluorescence values using non-linear regression analysis (curve fitting) in GraphPad Prism 9 (GraphPad Software Inc., USA).

Efficacy of CIP plus TQ combination therapy in SCID mice infected with *B. microti*

Twenty 6-week-old female immunocompromised mice (C.B-17/IcrJcl-Prkdcscid strain, CLEA Japan, Inc.) were intraperitoneally injected with 1.0×10^7 of *B. microti*-infected blood cells (Tuvshintulga et al., 2022). When the average parasitemia across all mice reached 1% (at 4 DPI), the drug treatments were initiated. The CIP group (n = 5) was orally administered 20 mg/kg CIP for seven days. The TQ group (n = 5) was orally administered a single dose of 20 mg/kg TQ. The CIP plus TQ group (n = 5) received the combination treatment, following the dosage and administration methods described above. The vehicle group (n = 5) orally received 0.2 mL of sesame oil as the control. Thin blood smears were prepared every other day and examined under a light microscope to determine parasitemia levels.

qPCR analysis

To further verify the presence or absence of *B. microti* DNA in treated SCID mice, real-time quantitative PCR analysis was performed as described previously (Vydyam et al., 2024). Briefly, genomic DNA was extracted from samples collected at 90 DPI and subjected to qPCR analysis using SYBR Green I, targeting a highly conserved region of *Babesia* mitochondrial genome (mtDNA). Primers used were: Bmic-F 5'-TTGCGATAGTAATAGATTTACTGC-3' and B-lsu-R2 5'-

TCTTAACCCAACTCACGTACCA-3' (Qurollo et al., 2017). The reaction mixture consisted of: 1 × Advanced Universal SYBR Green Super Mix (2 ×) (1725270; Bio-Rad); 0.5 µM of each primer, and 2 µl of genomic DNA.

Detection of *B. microti* ATP4 gene mutations in relapsed infected SCID mice

The genomic DNA of the mutant parasites was extracted and sequenced (Ji et al., 2022a). The primer sets used for sequencing are listed in **Table supplement 2**. The single nucleotide variants were confirmed by pairwise alignment to the *Bm*ATP4^{WT} sequence (GenBank: BMR1_03g01005).

Statistical analysis

Data analysis, namely one-way analysis of variance (ANOVA) and two-tailed unpaired t-tests, was performed using GraphPad Prism (La Jolla, CA, USA) version 9. A P value of <0.05 was considered a statistically significant result.

Supplementary Materials

Figure supplement 1.

Cytotoxicity assay of CIP on the Madin-Darby canine kidney (MDCK) cells and human foreskin fibroblasts (HFF).

The MTP-500 microplate reader is utilized to detect the absorbance at 450 nm. The results are displayed as the mean ± standard deviation of three separate tests. CC_{50}: the 50% cytotoxic concentration.

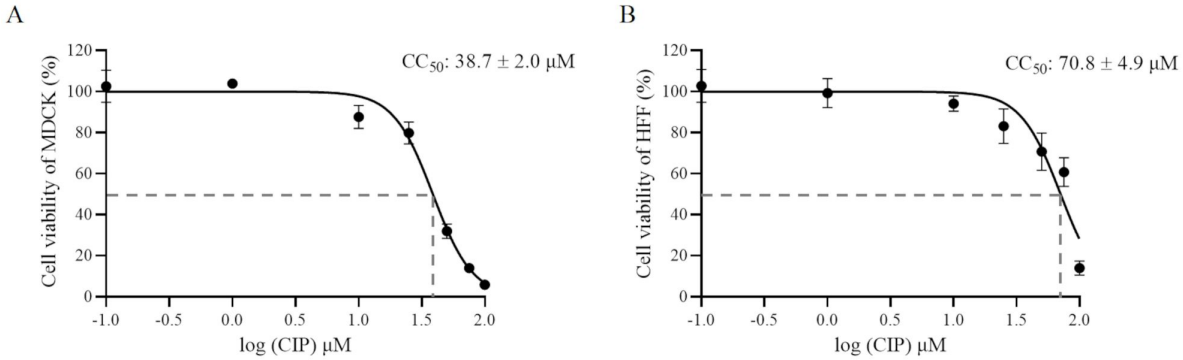

Figure supplement 2.

Multiple sequence alignment of ATP4 in different species.

A yellow square and arrow denotes the *Bg*ATP4 mutation site discovered in this investigation; purple squares and arrows represent sites linked to *P. falciparum* CIP resistance, and a gray square and arrow represents sites associated with *T. gondii*.

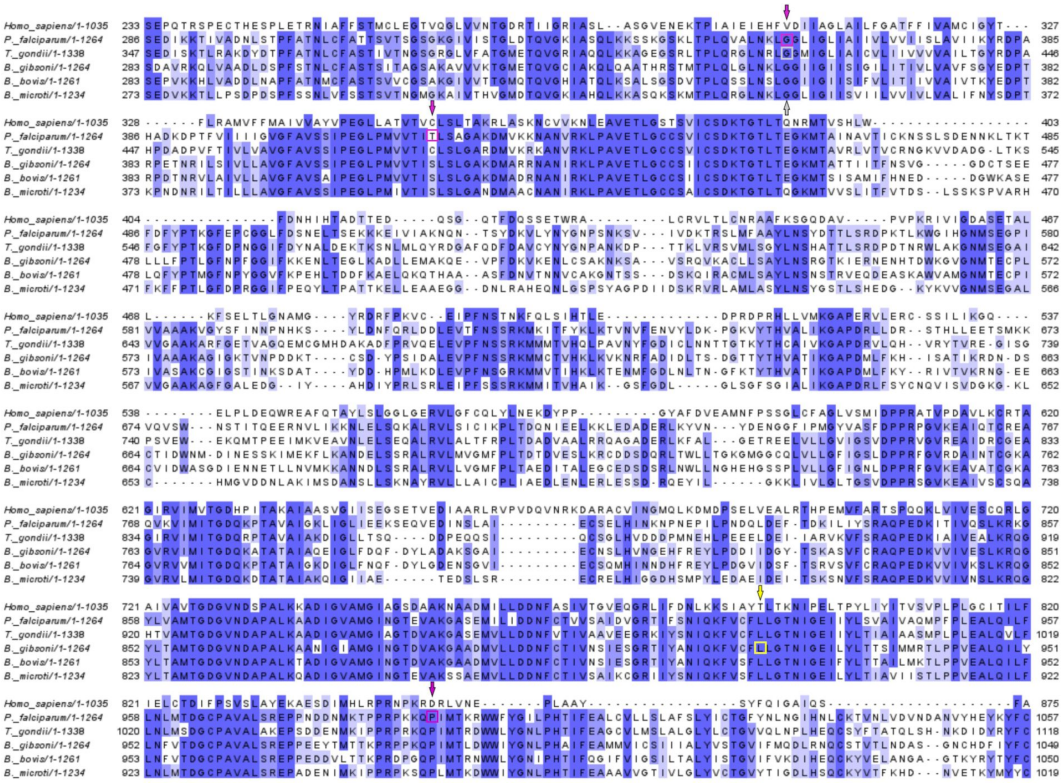

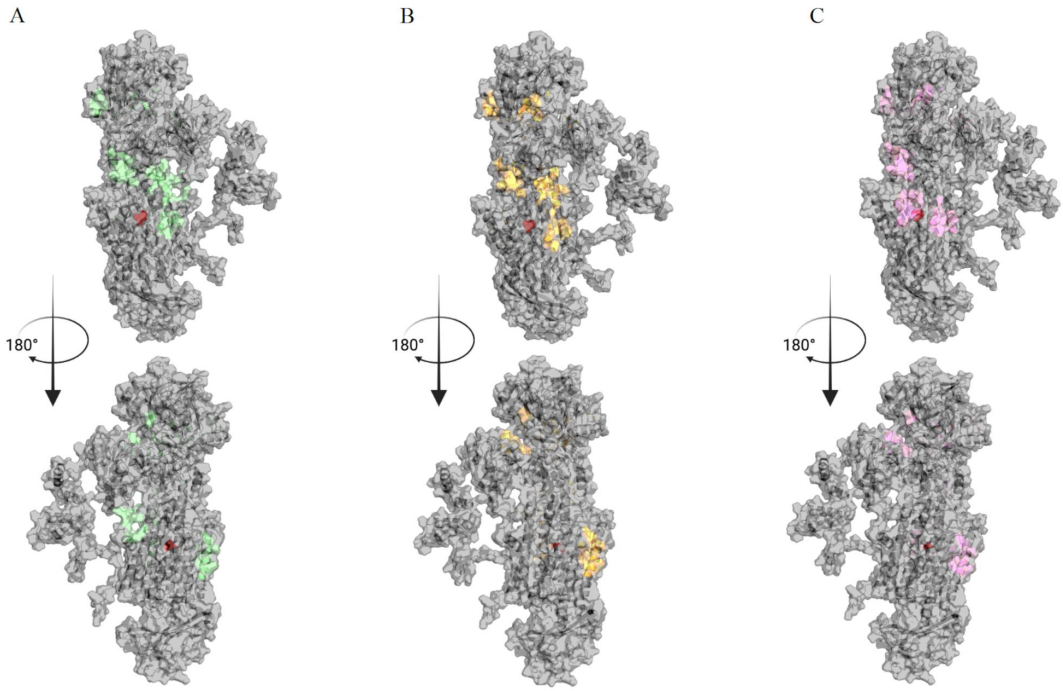

Figure supplement 3.

Binding sites for CIP found by Gnina search across the entire surface of the protein.

(**A**-**C**) The binding space of WT, L921V, and L921I mutants in *Bg*ATP4 are labeled in green, yellow and pink, respectively.

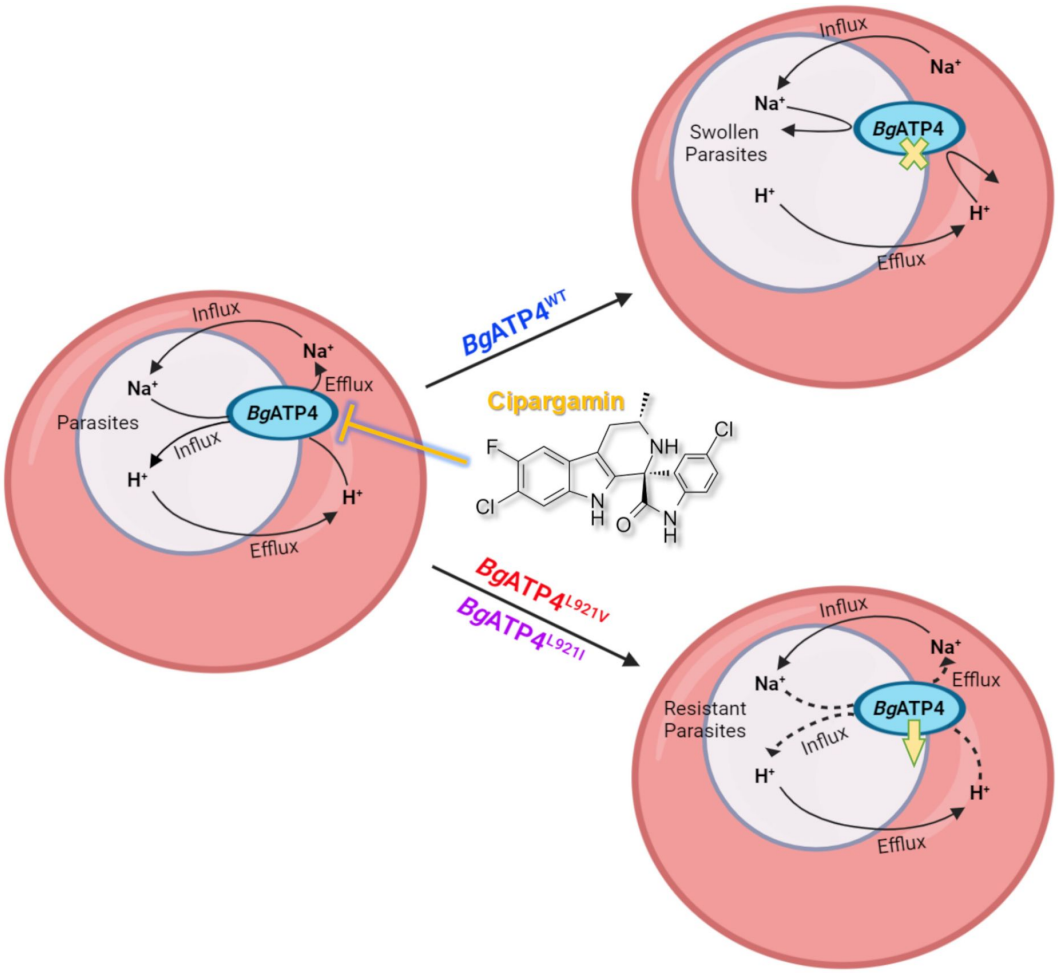

Figure supplement 4.

Proposed mechanism of inhibition of CIP on wild-type and mutant parasite-infected erythrocytes.

CIP disrupts the *Bg*ATP4 function of wild-type parasites, which causes a net influx of Na^+ and efflux of H^+ from the parasite. The osmotic load imposed on the influx of Na^+ further brings about parasite swelling and internal alkalinization, which are the main factors in *Babesia* death. Mutations in ATP4 minimize the susceptibility to ATP4 inhibitors by recovering H^+ and Na^+ balance, as indicated by the dotted arrows.

Supplemental Tables

Acknowledgements

This work was supported by a Grant-in-Aid for Scientific Research (22H0250906), the JSPS Core-to-Core program, both from the Ministry of Education, Culture, Sports, Science, and Technology of Japan, and a grant from the Strategic International Collaborative Research Project (JPJ008837) promoted by the Ministry of Agriculture, Forestry, and Fisheries of Japan, and International Science and Technology Cooperation Project of Hubei Province (2024EHA018).

Additional information

Author contributions

Hang Li, Investigation, Data curation, Formal analysis, Writing – original draft, Writing – review & editing; Shengwei Ji, Methodology, Investigation, Software, Validation; Nanang R. Ariefta, Methodology, Software, Formal analysis; Eloiza May S. Galon, Visualization, Writing – review & editing; Shimaa AES El-Sayed, Methodology, Visualization; Thom Do, Methodology, Investigation; Lijun Jia, Data curation, Visualization; Miako Sakaguchi, Methodology, Visualization; Masahito Asada, Investigation, Visualization; Yoshifumi Nishikawa, Methodology, Resources; Xin Qin, Methodology, Data curation; Mingming Liu, Conceptualization, Methodology, Investigation, Resources, Data curation, Funding acquisition, Supervision, Writing – review & editing; Xuenan Xuan, Conceptualization, Methodology, Validation, Formal analysis, Supervision, Project administration, Writing – review & editing.

Ethics

All animal experiments were performed according to the Guide for the Care and Use of Laboratory Animals of Obihiro University of Agriculture and Veterinary Medicine, which was also approved by the Committee on the Ethics of Animal Experiments at the Obihiro University of Agriculture and Veterinary Medicine, Japan (permit numbers: animal experiment, 22-145 and 23-132; DNA experiment, 2207 and 2208; pathogen, 202308 and 202306).

Gene	Primer (5'-3')
*Bg*ATP4-1F	ACGTAGTTGTCGAACATCTTACACCAATGC
*Bg*ATP4-1R	CAGAGGTAGCATAGTGAGATCGCCCCGA
*Bg*ATP4-2F	GAGATTGCAAGGTTTACGGATGAGTCTATGG
*Bg*ATP4-2R	ATGACAACGTCACCGGGTACAACACGCTTG
*Bg*ATP4-3F	GAAAAGCTTGCTCAAATGTCTTCACCGACAAC
*Bg*ATP4-3R	GTTTCTGGACGAGTTGGATCCTCATAACC
*Bg*ATP4-4F	AAATTGGGGGGGATAATTGGCATTATCTCC
*Bg*ATP4-4R	ACCTTATCAAAGGGTACCTCTTGCTTTG
*Bg*ATP4-5F	TCAATCCATTCGGTGGAATTTTCAAAAAGG
*Bg*ATP4-5R	GTGTTTGAATAACATATCTGGTGCCCCCTT
*Bg*ATP4-6F	GGTAAAGAACAGATTTGCTGACATAGATCT
*Bg*ATP4-6R	ACCCTATTTCTTGTGCGATGGCCGTAGCTG
*Bg*ATP4-7F	AGGGACGCTATAAATACTTGTGGAAAGGC
*Bg*ATP4-7R	GTACGCCCAGACTCGATTGAGTTAACTATTG
*Bg*ATP4-8F	GGGTATTAATGGCACAGATGTTGCAAAAGG
*Bg*ATP4-8R	GACAGTTCCCACTAGCATCATTAAGTGTAA
*Bg*ATP4-9F	ATCATCATTGCGCTATATGTTTCTACCGG
*Bg*ATP4-9R	CTAATGGGGTAGCATTTCCATTCTCAACAA
*Bg*ATP4-10F	AGGGAGTTCCTCCCATGTATAAAGATACCT
*Bg*ATP4 10R	TTAGGCTTCTGCCCTTTTCATTTTTCGCTT

Table supplement 1.

Primer sets of *B. gibsoni* ATP4

Gene	Primer (5'-3')
*Bm*ATP4-1F	ATGAGTAGATCTCAGTCTAACATTTC
*Bm*ATP4-1R	TGCTATTAGTAGTGCTATAACAAAG
*Bm*ATP4-2F	CAAGTATGGCGAAAATGCTATAAAC
*Bm*ATP4-2R	CATTCCGTTTGTTACGCTGGTGC
*Bm*ATP4-3F	CTTACAGGTGAGAGTGAAGATGTAAAG
*Bm*ATP4-3R	ACAAATTGCTGAGCAGCAACCCAGAG
*Bm*ATP4-4F	CTATTTCATTGTCATTGGGAGCTAA
*Bm*ATP4-4R	CAAATCCGGCCTTAGCTGCGCCAA
*Bm*ATP4-5F	TCATACGGTTCAACGTTATCACATG
*Bm*ATP4-5R	TCTATCCGACGACTCCAACCTTTC
*Bm*ATP4-6F	GTTGTCCAAGAATGCTTATAGGGTG
*Bm*ATP4-6R	CATTGCCACGCCAATGTCCGCCTGTTT
*Bm*ATP4-7F	GTTAACTCGTTGAAGAGACAAGGTTAC
*Bm*ATP4-7R	CACAATTGTACCGACAACTGCCGCTG
*Bm*ATP4-8F	GGCCAAAATCTCAGCCTTTAATGAC
*Bm*ATP4-8R	CAGCTCCAATGGGTTGGTAGTAACCATT
*Bm*ATP4-9F	CGTTATTGACGGCGTTGAGAATGATG
*Bm*ATP4-9R	CCCAAAACACCTTTGCCATTTAACTC
*Bm*ATP4-10F	GAAAATTGTAGAGCATTTCAAAACCAG
*Bm*ATP4 10R	TTATTGCAGGGCAGCCTGCTTAGA

Table supplement 2.

Primer sets of *B. microti* ATP4

Receptor and binding energy	Name	Distance	Category	Types
*Bg*ATP4^{WT} -6.43 kcal/mol	GLY407	2.67648	Hydrogen Bond; Halogen	Carbon Hydrogen Bond; Halogen (Fluorine)
	CYS959	3.2396	Halogen	Halogen (Cl, Br, I)
	VAL962	2.66882	Hydrophobic	Pi-Sigma
	CYS959	4.38742	Hydrophobic	Alkyl
	VAL962	4.29249	Hydrophobic	Alkyl
	ALA963	3.8231	Hydrophobic	Alkyl
	ALA1202	3.67015	Hydrophobic	Alkyl
	MET211	5.06565	Hydrophobic	Alkyl
	VAL962	4.25668	Hydrophobic	Alkyl
	ILE414	4.70605	Hydrophobic	Alkyl
	CYS959	4.83891	Hydrophobic	Pi-Alkyl
	VAL962	4.98402	Hydrophobic	Pi-Alkyl
	VAL411	5.43239	Hydrophobic	Pi-Alkyl
	VAL962	5.05537	Hydrophobic	Pi-Alkyl
	PHE954	4.07586	Hydrophobic	Pi-Alkyl
*Bg*ATP4^{L921V} -6.40 kcal/mol	GLY407	2.69013	Hydrogen Bond; Halogen	Carbon Hydrogen Bond; Halogen (Fluorine)
	CYS959	3.22066	Halogen	Halogen (Cl, Br, I)
	VAL962	2.66391	Hydrophobic	Pi-Sigma
	CYS959	4.35422	Hydrophobic	Alkyl
	VAL962	4.31879	Hydrophobic	Alkyl
	ALA963	3.8209	Hydrophobic	Alkyl
	ALA1202	3.63038	Hydrophobic	Alkyl
	MET211	5.0878	Hydrophobic	Alkyl
	VAL962	4.24186	Hydrophobic	Alkyl
	ILE414	4.71819	Hydrophobic	Alkyl
	CYS959	4.82036	Hydrophobic	Pi-Alkyl
	VAL962	4.99879	Hydrophobic	Pi-Alkyl
	VAL411	5.4334	Hydrophobic	Pi-Alkyl
	VAL962	5.04532	Hydrophobic	Pi-Alkyl
	PHE954	4.07482	Hydrophobic	Pi-Alkyl
	GLY958	2.92346	Hydrogen Bond; Halogen	Carbon Hydrogen Bond; Halogen (Fluorine)
	GLY958	3.3301	Halogen	Halogen (Fluorine)
	MET410	5.88505	Other	Pi-Sulfur

Table supplement 3.

Interactions of CIP from docking simulations

	VAL955	4.31406	Hydrophobic	Alkyl
	MET410	3.69023	Hydrophobic	Alkyl
*Bg*ATP4^{L921I}	VAL411	4.83101	Hydrophobic	Alkyl
-6.26 kcal/mol	VAL955	4.79513	Hydrophobic	Alkyl
	VAL955	4.84729	Hydrophobic	Alkyl
	CYS959	4.1269	Hydrophobic	Alkyl
	ILE1205	4.82529	Hydrophobic	Alkyl
	CYS959	5.21399	Hydrophobic	Alkyl
	VAL955	4.90527	Hydrophobic	Pi-Alkyl
	PHE954	5.03012	Hydrophobic	Pi-Alkyl

Table supplement 3. (continued)

References

Almazán C, Scimeca RC, Reichard MV, Mosqueda J 2022) **Babesiosis and Theileriosis in North America** *Pathogens* **11**:168 https://doi.org/10.3390/pathogens11020168

Ariefta NR, Pagmadulam B, Nihei C, Nishikawa Y 2022) **Sparsomycin exhibits potent antiplasmodial activity in vitro and in vivo** *Pharmaceutics* **14**:544 https://doi.org/10.3390/pharmaceutics14030544

Bork S, Yokoyama N, Matsuo T, Claveria FG, Fujisaki K, Igarashi I 2003) **Clotrimazole, ketoconazole, and clodinafop-propargyl inhibit the in vitro growth of Babesia bigemina and Babesia bovis (Phylum Apicomplexa)** *Parasitology* **127**:311–315 https://doi.org/10.1017/S0031182003003895

Carvalho LJM, Tuvshintulga B, Nugraha AB, Sivakumar T, Yokoyama N 2020) **Activities of artesunate-based combinations and tafenoquine against Babesia bovis in vitro and Babesia microti in vivo** *Parasites Vectors* **13**:362 https://doi.org/10.1186/s13071-020-04235-7

Chu CS, Freedman DO 2019) **Tafenoquine and G6PD: a primer for clinicians** *J Travel Med* **26** https://doi.org/10.1093/jtm/taz023

ClinicalTrials.gov [Internet]. Bethesda (MD): National Library of Medicine (US) 2024) **Identifier NCT04675931, To evaluate efficacy, safety, tolerability and PK of intravenous cipargamin in participants with severe Plasmodium falciparum malaria** https://clinicaltrials.gov/study/NCT04675931

Das S, Bhatanagar S, Morrisey JM, Daly TM, Burns JM, Coppens I, Vaidya AB 2016) **Na+ influx induced by new antimalarials causes rapid alterations in the cholesterol content and morphology of Plasmodium falciparum** *PLoS Pathog* **12**:e1005647 https://doi.org/10.1371/journal.ppat.1005647

Dennis ASM, Lehane AM, Ridgway MC, Holleran JP, Kirk K 2018) **Cell swelling induced by the antimalarial KAE609 (cipargamin) and other PfATP4-associated antimalarials** *Antimicrob Agents Chemother* **62**:e00087–18 https://doi.org/10.1128/AAC.00087-18

Diarra A, Sheldon C, Church J 2001) **In situ calibration and [H+] sensitivity of the fluorescent Na+ indicator SBFI** *American Journal of Physiology-Cell Physiology* **280**:C1623–C1633 https://doi.org/10.1152/ajpcell.2001.280.6.C1623

Eberhardt J, Santos-Martins D, Tillack AF, Forli S 2021) **AutoDock Vina 1.2.0: new docking methods, expanded force field, and python bindings** *J Chem Inf Model* **61**:3891–3898 https://doi.org/10.1021/acs.jcim.1c00203

Gray JS, Ogden NH 2021) **Ticks, human babesiosis and climate change** *Pathogens* **10**:1430 https://doi.org/10.3390/pathogens10111430

Guswanto A, Sivakumar T, Rizk MA, Elsayed SAE, Youssef MA, ElSaid EES, Yokoyama N, Igarashi I 2014) **Evaluation of a fluorescence-based method for antibabesial drug screening** *Antimicrob Agents Chemother* **58**:4713–4717 https://doi.org/10.1128/AAC.00022-14

Hidayati AR, Melinda Ilmi H, Sakura T, Sakaguchi M, Ohmori J, Hartuti ED, Tumewu L, Inaoka DK, Tanjung M, Yoshida E, Tokumasu F, Kita K, Mori M, Dobashi K, Nozaki T, Syafruddin D, Hafid AF, Waluyo D, Widyawaruyanti A 2023) **Effect of geranylated dihydrochalcone from Artocarpus altilis leaves extract on Plasmodium falciparum ultrastructural changes and mitochondrial malate: Quinone oxidoreductase** *International Journal for Parasitology: Drugs and Drug Resistance* **21**:40–50 https://doi.org/10.1016/j.ijpddr.2022.12.001

Holbrook NR, Klontz EH, Adams GC, Schnittman SR, Issa NC, Bond SA, Branda JA, Lemieux JE 2023) **Babesia microti variant with multiple resistance mutations detected in an immunocompromised patient receiving atovaquone prophylaxi** *Open Forum Infectious Diseases* **10**:ofad097 https://doi.org/10.1093/ofid/ofad097

Hwang S-J, Yamasaki M, Nakamura K, Sasaki N, Murakami M, Wickramasekara Rajapakshage BK, Ohta H, Maede Y, Takiguchi M 2010) **Development and characterization of a strain of Babesia gibsoni resistant to diminazene aceturate in vitro** *J Vet Med Sci* **72**:765–771 https://doi.org/10.1292/jvms.09-0535

Jalovecka M, Sojka D, Ascencio M, Schnittger L 2019) **Babesia life cycle-when phylogeny meets biology** *Trends in Parasitology* **35**:356–368 https://doi.org/10.1016/j.pt.2019.01.007

Jeon SA, Park JL, Park S-J, Kim JH, Goh S-H, Han J-Y, Kim S-Y 2021) **Comparison between MGI and Illumina sequencing platforms for whole genome sequencing** *Genes Genom* **43**:713–724 https://doi.org/10.1007/s13258-021-01096-x

Ji S, Galon EM, Rizk MA, Yi Y, Zafar I, Li H, Ma Z, Iguchi A, Asada M, Liu M, Xuan X 2022a) **Efficacy of the antimalarial MMV390048 against Babesia infection reveals phosphatidylinositol 4-kinase as a druggable target for babesiosis** *Antimicrob Agents Chemother* **66**:e00574–22 https://doi.org/10.1128/aac.00574-22

Ji S, Liu M, Galon EM, Rizk MA, Tuvshintulga B, Li J, Zafar I, Hasegawa Y, Iguchi A, Yokoyama N, Xuan X 2022b) **Inhibitory effect of naphthoquine phosphate on Babesia gibsoni in vitro and Babesia rodhaini in vivo** *Parasites Vectors* **15**:10 https://doi.org/10.1186/s13071-021-05127-0

Jo S, Cheng X, Islam SM, Huang L, Rui H, Zhu A, Lee HS, Qi Y, Han W, Vanommeslaeghe K, MacKerell AD, Roux B, Im W 2014) **CHARMM-GUI PDB manipulator for advanced modeling and simulations of proteins containing nonstandard residues** *Adv Protein Chem Struct Biol* **96**:235–265 https://doi.org/10.1016/bs.apcsb.2014.06.002

Jumper J, Evans R, Pritzel A, Green T, Figurnov M, Ronneberger O, Tunyasuvunakool K, Bates R, Žídek A, Potapenko A, Bridgland A, Meyer C, Kohl SAA, Ballard AJ, Cowie A, Romera-Paredes B, Nikolov S, Jain R, Adler J, Back T, et al. 2021) **Highly accurate protein structure prediction with AlphaFold** *Nature* **596**:583–589 https://doi.org/10.1038/s41586-021-03819-2

Kletsova EA, Spitzer ED, Fries BC, Marcos LA 2017) **Babesiosis in Long Island: review of 62 cases focusing on treatment with azithromycin and atovaquone** *Ann Clin Microbiol Antimicrob* **16**:26 https://doi.org/10.1186/s12941-017-0198-9

Krause PJ 2019) **Human babesiosis** *International Journal for Parasitology* **49**:165–174 https://doi.org/10.1016/j.ijpara.2018.11.007

Krause PJ, Auwaerter PG, Bannuru RR, Branda JA, Falck-Ytter YT, Lantos PM, Lavergne V, Meissner HC, Osani MC, Rips JG, Sood SK, Vannier E, Vaysbrot EE, Wormser GP 2021) **Clinical practice guidelines by the infectious diseases society of America (IDSA): 2020 guideline**

on diagnosis and management of babesiosis *Clinical Infectious Diseases* **72**:e49–e64 https://doi.org/10.1093/cid/ciaa1216

Krause PJ, Rogers R, Shah MK, Kang H, Parsonnet J, Kodama R, Vannier E 2024) **Tafenoquine for relapsing babesiosis: a case series** *Clinical Infectious Diseases* **79**:130–137 https://doi.org/10.1093/cid/ciae238

Krishna S, Woodrow C, Webb R, Penny J, Takeyasu K, Kimura M, East JM 2001) **Expression and functional characterization of a Plasmodium falciparum Ca2+-ATPase (PfATP4) belonging to a subclass unique to apicomplexan organisms** *Journal of Biological Chemistry* **276**:10782–10787 https://doi.org/10.1074/jbc.M010554200

Lee AH, Fidock DA 2016) **Evidence of a mild mutator phenotype in cambodian Plasmodium falciparum malaria parasites** *PLoS ONE* **11**:e0154166 https://doi.org/10.1371/journal.pone.0154166

Lehane AM, Dennis ASM, Bray KO, Li D, Rajendran E, McCoy JM, McArthur HM, Winterberg M, Rahimi F, Tonkin CJ, Kirk K, Van Dooren GG. 2019) **Characterization of the ATP4 ion pump in Toxoplasma gondii** *Journal of Biological Chemistry* **294**:5720–5734 https://doi.org/10.1074/jbc.RA118.006706

Lemieux JE, Tran AD, Freimark L, Schaffner SF, Goethert H, Andersen KG, Bazner S, Li A, McGrath G, Sloan L, Vannier E, Milner D, Pritt B, Rosenberg E, Telford S, Bailey JA, Sabeti PC 2016) **A global map of genetic diversity in Babesia microti reveals strong population structure and identifies variants associated with clinical relapse** *Nat Microbiol* **1**:16079 https://doi.org/10.1038/nmicrobiol.2016.79

Li H, Galon EM, Ji S, Zafar I, Ma Z, Do T, Amer MM, Ma Y, Liu M, Xuan X 2023) **In vitro screening of compounds from the Food and Drug Administration-approved library identifies anti-Babesia gibsoni activity of idarubicin hydrochloride and vorinostat** *Parasitology International* **96**:102774 https://doi.org/10.1016/j.parint.2023.102774

Lindahl Abraham, Hess Spoel VD 2021) **GROMACS 2021 Manual** *Zenodo* https://doi.org/10.5281/ZENODO.4457591

Liu M, Adjou Moumouni PF, Cao S, Asada M, Wang G, Gao Y, Guo H, Li J, Vudriko P, Efstratiou A, Ringo AE, Lee S-H, Hakimi H, Masatani T, Sunaga F, Kawazu S, Yamagishi J, Jia L, Inoue N, Xuan X 2018) **Identification and characterization of interchangeable cross-species functional promoters between Babesia gibsoni and Babesia bovis** *Ticks and Tick-borne Diseases* **9**:330–333 https://doi.org/10.1016/j.ttbdis.2017.11.008

Liu M, Galon EM, Ji S, Xuan X 2024) **Tafenoquine-based combination therapies: a step toward babesiosis elimination** *The Journal of Infectious Diseases* **229**:1599–1600 https://doi.org/10.1093/infdis/jiae083

Liu M, Ji S, Kondoh D, Galon EM, Li J, Tomihari M, Yanagawa M, Tagawa M, Adachi M, Asada M, Igarashi I, Iguchi A, Xuan X 2021) **Tafenoquine is a promising drug candidate for the treatment of babesiosis** *Antimicrob Agents Chemother* **65**:e00204–21 https://doi.org/10.1128/AAC.00204-21

Marcos LA, Leung A, Kirkman L, Wormser GP 2022) **Use of tafenoquine to treat a patient with relapsing babesiosis with clinical and molecular evidence of resistance to azithromycin and atovaquone** *IDCases* **27**:e01460 https://doi.org/10.1016/j.idcr.2022.e01460

Matsuu A, Koshida Y, Kawahara M, Inoue K, Ikadai H, Hikasa Y, Okano S, Higuchi S 2004) **Efficacy of atovaquone against Babesia gibsoni in vivo and in vitro** *Veterinary Parasitology* **124**:9–18 https://doi.org/10.1016/j.vetpar.2004.07.005

Mohring F, Van Schalkwyk DA, Henrici RC, Blasco B, Leroy D, Sutherland CJ, Moon RW. 2022) **Cation ATPase (ATP4) orthologue replacement in the malaria parasite Plasmodium knowlesi reveals species-specific responses to ATP4-targeting drugs** *mBio* **13**:e01178–22 https://doi.org/10.1128/mbio.01178-22

Ndayisaba G, Yeka A, Asante KP, Grobusch MP, Karita E, Mugerwa H, Asiimwe S, Oduro A, Fofana B, Doumbia S, Jain JP, Barsainya S, Kullak-Ublick GA, Su G, Schmitt EK, Csermak K, Gandhi P, Hughes D 2021) **Hepatic safety and tolerability of cipargamin (KAE609), in adult patients with Plasmodium falciparum malaria: a randomized, phase II, controlled, dose-escalation trial in sub-Saharan Africa** *Malar J* **20**:478 https://doi.org/10.1186/s12936-021-04009-1

Qiu D, Pei JV, Rosling JEO, Thathy V, Li D, Xue Y, Tanner JD, Penington JS, Aw YTV, Aw JYH, Xu G, Tripathi AK, Gnadig NF, Yeo T, Fairhurst KJ, Stokes BH, Murithi JM, Kümpornsin K, Hasemer H, Dennis ASM, et al. 2022) **A G358S mutation in the Plasmodium falciparum Na+ pump PfATP4 confers clinically-relevant resistance to cipargamin** *Nat Commun* **13**:5746 https://doi.org/10.1038/s41467-022-33403-9

Qurollo BA, Archer NR, Schreeg ME, Marr HS, Birkenheuer AJ, Haney KN, Thomas BS, Breitschwerdt EB 2017) **Improved molecular detection of Babesia infections in animals using a novel quantitative real-time PCR diagnostic assay targeting mitochondrial DNA** *Parasites Vectors* **10**:128 https://doi.org/10.1186/s13071-017-2064-1

Rogers R, Krause PJ, Norris AM, Ting MH, Nagami EH, Cilley B, Vannier E 2023) **Broad antimicrobial resistance in a case of relapsing babesiosis successfully treated with tafenoquine** *Clinical Infectious Diseases* **76**:741–744 https://doi.org/10.1093/cid/ciac473

Rosenblatt J, Leung A, Baneman E, Fuller R, Taimur S, Paniz-Mondolfi AE, Malone AK, Kirkman L, Jacobs SE 2021) **Relapsed Babesia microti infection following allogeneic hematopoietic cell transplantation in a patient with B-cell acute lymphoblastic leukemia: case report and review of the literature** *Open Forum Infectious Diseases* **8**:ofab323 https://doi.org/10.1093/ofid/ofab323

Rosling JEO, Ridgway MC, Summers RL, Kirk K, Lehane AM 2018) **Biochemical characterization and chemical inhibition of PfATP4-associated Na+-ATPase activity in Plasmodium falciparum membranes** *Journal of Biological Chemistry* **293**:13327–13337 https://doi.org/10.1074/jbc.RA118.003640

Rottmann M, McNamara C, Yeung BKS, Lee MCS, Zou B, Russell B, Seitz P, Plouffe DM, Dharia NV, Tan J, Cohen SB, Spencer KR, González-Páez GE, Lakshminarayana SB, Goh A, Suwanarusk R, Jegla T, Schmitt EK, Beck H-P, Brun R, et al. 2010) **Spiroindolones, a potent compound class for the treatment of malaria** *Science* **329**:1175–1180 https://doi.org/10.1126/science.1193225

Saliba KJ, Kirk K 1999) **pH regulation in the intracellular malaria parasite, Plasmodium falciparum** *Journal of Biological Chemistry* **274**:33213–33219 https://doi.org/10.1074/jbc.274.47.33213

Schmitt EK, Ndayisaba G, Yeka A, Asante KP, Grobusch MP, Karita E, Mugerwa H, Asiimwe S, Oduro A, Fofana B, Doumbia S, Su G, Csermak Renner K, Venishetty VK, Sayyed S, Straimer J, Demin I, Barsainya S, Boulton C, Gandhi P 2022) **Efficacy of cipargamin (KAE609) in a**

randomized, phase II dose-escalation study in adults in Sub-Saharan Africa with uncomplicated Plasmodium falciparum malaria *Clinical Infectious Diseases* **74**:1831–1839 https://doi.org/10.1093/cid/ciab716

Simon MS, Westblade LF, Dziedziech A, Visone JE, Furman RR, Jenkins SG, Schuetz AN, Kirkman LA 2017) **Clinical and molecular evidence of atovaquone and azithromycin resistance in relapsed Babesia microti infection associated with rituximab and chronic lymphocytic leukemia** *Clinical Infectious Diseases* **65**:1222–1225 https://doi.org/10.1093/cid/cix477

Spillman NJ, Allen RJW, McNamara CW, Yeung BKS, Winzeler EA, Diagana TT, Kirk K. 2013) **Na+ regulation in the malaria parasite Plasmodium falciparum involves the cation ATPase PfATP4 and is a target of the spiroindolone antimalarials** *Cell Host & Microbe* **13**:227–237 https://doi.org/10.1016/j.chom.2012.12.006

Tayebwa DS, Tuvshintulga B, Guswanto A, Nugraha AB, Batiha GE-S, Gantuya S, Rizk MA, Vudriko P, Sivakumar T, Yokoyama N, Igarashi I 2018) **The effects of nitidine chloride and camptothecin on the growth of Babesia and Theileria parasites** *Ticks and Tick-borne Diseases* **9**:1192–1201 https://doi.org/10.1016/j.ttbdis.2018.04.019

Trott O, Olson AJ 2010) **AutoDock Vina: improving the speed and accuracy of docking with a new scoring function, efficient optimization, and multithreading** *J Comput Chem* **31**:455–461 https://doi.org/10.1002/jcc.21334

Tuvshintulga B, Sivakumar T, Nugraha AB, Ahedor B, Batmagnai E, Otgonsuren D, Liu M, Xuan X, Igarashi I, Yokoyama N 2022) **Combination of clofazimine and atovaquone as a potent therapeutic regimen for the radical cure of Babesia microti infection in immunocompromised hosts** *The Journal of Infectious Diseases* **225**:238–242 https://doi.org/10.1093/infdis/jiab537

Vannier E, Krause PJ 2012) **Human babesiosis** *N Engl J Med* **366**:2397–2407 https://doi.org/10.1056/NEJMra1202018

Vega CA, Buening GM, Green TJ, Carson CA 1985) **In vitro cultivation of Babesia bigemina** *Am J Vet Res* **46**:416–420

Vydyam P, Pal AC, Renard I, Chand M, Kumari V, Gennaro JC, Mamoun CB 2024) **Tafenoquine-atovaquone combination achieves radical cure and confers sterile immunity in experimental models of human babesiosis** *The Journal of Infectious Diseases* **229**:161–172 https://doi.org/10.1093/infdis/jiad315

Zhang R, Suwanarusk R, Malleret B, Cooke BM, Nosten F, Lau Y-L, Dao M, Lim CT, Renia L, Tan KSW, Russell B 2016) **A basis for rapid clearance of circulating ring-stage malaria parasites by the spiroindolone KAE609** *J Infect Dis* **213**:100–104 https://doi.org/10.1093/infdis/jiv358

Zhou Y, Fomovska A, Muench S, Lai B-S, Mui E, McLeod R 2014) **Spiroindolone that inhibits PfATPase4 is a potent, cidal inhibitor of Toxoplasma gondii tachyzoites in vitro and in vivo** *Antimicrob Agents Chemother* **58**:1789–1792 https://doi.org/10.1128/AAC.02225-13

Author information

Hang Li[†]
National Research Center for Protozoan Diseases, Obihiro University of Agriculture Veterinary Medicine, Obihiro, Japan

[†]These authors contributed equally to this work.

Shengwei Ji[†]
National Research Center for Protozoan Diseases, Obihiro University of Agriculture Veterinary Medicine, Obihiro, Japan, Department of Veterinary Medicine, Agriculture College of Yanbian University, Yanji, China

[†]These authors contributed equally to this work.

Nanang R Ariefta
National Research Center for Protozoan Diseases, Obihiro University of Agriculture Veterinary Medicine, Obihiro, Japan

Eloiza May S Galon
College of Veterinary Medicine and Biomedical Sciences, Cavite State University, Indang, Philippines

Shimaa AES El-Sayed
National Research Center for Protozoan Diseases, Obihiro University of Agriculture Veterinary Medicine, Obihiro, Japan, Department of Biochemistry and Molecular Biology, Faculty of Veterinary Medicine, Mansoura University, Mansoura Egypt

Thom Do
National Research Center for Protozoan Diseases, Obihiro University of Agriculture Veterinary Medicine, Obihiro, Japan

Lijun Jia
Department of Veterinary Medicine, Agriculture College of Yanbian University, Yanji, China

Miako Sakaguchi
Central Laboratory, Institute of Tropical Medicine (NEKKEN), Nagasaki University, Nagasaki, Japan

Masahito Asada
National Research Center for Protozoan Diseases, Obihiro University of Agriculture Veterinary Medicine, Obihiro, Japan

Yoshifumi Nishikawa
National Research Center for Protozoan Diseases, Obihiro University of Agriculture Veterinary Medicine, Obihiro, Japan

Xin Qin
School of Basic Medicine, Hubei University of Arts and Science, Xiangyang, China

Mingming Liu
School of Basic Medicine, Hubei University of Arts and Science, Xiangyang, China
ORCID iD: 0000-0003-2780-110X

For correspondence: lmm_2010@hotmail.com

Xuenan Xuan
National Research Center for Protozoan Diseases, Obihiro University of Agriculture Veterinary Medicine, Obihiro, Japan

For correspondence: gen@obihiro.ac.jp

Editors

Reviewing Editor
Warren Andrew Andayi
Murang'a University of Technology, Murang'a, Kenya

Senior Editor
Dominique Soldati-Favre
University of Geneva, Geneva, Switzerland

Reviewer #2 (Public review):

Summary:

In this manuscript, authors have tried to repurpose cipargamin (CIP), a known drug against Plasmodium and Toxoplasma against Babesia. They proved the efficacy of CIP on Babesia in nanomolar range. In silico analyses revealed the drug resistance mechanism through a single amino acid mutation at amino acid position 921 on the ATP4 gene of Babesia. Overall, the conclusions drawn by the authors are well justified by their data. I believe this study opens up a novel therapeutic strategy against babesiosis.

Strengths:

Authors have carried out a comprehensive study. All the experiments performed were carried out methodically and logically.

https://doi.org/10.7554/eLife.101128.2.sa2

Reviewer #3 (Public review):

Summary:

The authors aim to establish that cipargamin can be used for the treatment of infection caused by Babesia organisms.

Strengths:

The study provides strong evidence that cipargamin is effective against various Babesia species. In vitro growth assays were used to establish that cipargamin is effective against Babesia bovis and Babesia gibsoni. Infection of mice with Babesia microti demonstrated that cipargamin is as effective as the combination of atovaquone plus azithromycin. Cipargamin protected mice from lethal infection with Babesia rodhaini. Mutations that confer resistance

to cipargamin were identified in the gene encoding ATP4, a P-type Na ATPase that is found in other apicomplexan parasites, thereby validating ATP4 as the target of cipargamin. A 7-day treatment of cipagarmin, when combined with a single dose of tafenoquine, was sufficient to eradicate Babesia microti in a mouse model of severe babesiosis caused by lack of adaptive immunity.

Weaknesses:

Cipargamin was tested in vivo at a single dose administered daily for 7 days. Despite the prospect of using cipargamin for the treatment of human babesiosis, there was no attempt to identify the lowest dose of cipagarmin that protects mice from Babesia microti infection. In the SCID mouse model, cipargamin was tested in combination with tafenoquine but not with atovaquone and/or azithromycin, although the latter combination is often used as first-line therapy for human babesiosis caused by Babesia microti.

https://doi.org/10.7554/eLife.101128.2.sa1

Author response:

The following is the authors' response to the original reviews.

> ***Public Reviews:***
>
> ***Reviewer #1 (Public review):***
>
> *Summary:*
>
> *In this manuscript, the authors address an important issue in* Babesia *research by repurposing cipargamin (CIP) as a potential therapeutic against selective* Babesia *spp. In this study, CIP demonstrated potent* in vitro *inhibition of* B. bovis *and* B. gibsoni *with* IC_{50} *values of 20.2 ± 1.4 nM and 69.4 ± 2.2 nM, respectively, and the* in vivo *efficacy against* Babesia *spp. using mouse model. The authors identified two key resistance mutations in the BgATP4 gene (BgATP4*^{L921I} *and BgATP4*^{L921V}*) and explored their implications through phenotypic characterization of the parasite using cell biological experiments, complemented by* in silico *analysis. Overall, the findings are promising and could significantly advance* Babesia *treatment strategies.*
>
> *Strengths:*
>
> *In this manuscript, the authors effectively repurpose cipargamin (CIP) as a potential treatment for* Babesia *spp. They provide compelling* in vitro *and* in vivo *data showing strong efficacy. Key resistance mutations in the BgATP4 gene are identified and analyzed through both phenotypic and in silico methods, offering valuable insights for advancing treatment strategies.*

Thank you for your insightful comments and for taking the time to review our manuscript.

Weaknesses:

> *The manuscript explores important aspects of drug repurposing and rational drug design using cipargamin (CIP) against* Babesia*. However, several weaknesses should be addressed. The study lacks novelty as similar research on cipargamin has been conducted, and the experimental design could be improved. The rationale for choosing CIP over other ATP4-targeting compounds is not well-explained. Validation of mutations relies heavily on* in silico *predictions without sufficient experimental support. The Ion Transport Assay has limitations and would benefit from additional assays like*

> *Radiolabeled Ion Flux and Electrophysiological Assays. Also, the study lacks appropriate control drugs and detailed functional characterization. Further clarity on mutation percentages, additional safety testing, and exploration of cross-resistance would strengthen the findings.*

We appreciate your feedback and for giving us the chance to improve our paper. We have specified how we revised the below comments one by one. I hope these address your concerns.

> *Comment 1: It is commendable to explore drug repurposing, drug deprescribing, drug repositioning, and rational drug design, especially using established ATP4 inhibitors that are well-studied in* Plasmodium *and other protozoan parasites. While the study provides some interesting findings, it appears to lack novelty, as similar investigations of cipargamin on other protozoan parasites have been conducted. The study does not introduce new concepts, and the experimental design could benefit from refinement to strengthen the results. Additionally, the rationale for choosing CIP over other MMV compounds targeting ATP4 is not clearly articulated. Clarifying the specific advantages CIP may offer against* Babesia *would be beneficial. Finally, the validation of the identified mutations might be strengthened by additional experimental support, as reliance on* in silico *predictions alone may not fully address the functional impact, particularly given the potential ambiguity of the mutations (BgATP4 L to V and I).*

Thank you for your thoughtful feedback. We have addressed the concerns as follows: (1) Introduction of new concepts and experimental design: While our study primarily builds on existing frameworks, it provides novel insights into the interaction of CIP with *Babesia* parasites, which we believe contribute to the field. Regarding the experimental design, we acknowledge its limitations and have revised the manuscript to include additional experiments to strengthen the robustness of our findings. Specifically, we have added experiments on the detection of *Bg*ATP4-associated ATPase activity (Figure 3H), the evaluation of cross-resistance to antibabesial agents (Figures 5A and 5B), and the efficacy of CIP plus TQ combination in eliminating *B. microti* infection with no recrudescence in SCID mice (Figure 5C).

(2) Rationale for choosing CIP over other MMV compounds targeting ATP4: We appreciate this point and have expanded the introduction section to articulate our rationale for selecting CIP (Lines 94-97). Specifically, CIP was chosen due to its previously demonstrated efficacy against *Plasmodium* and other protozoan parasites.

(3) Validation of identified mutations: We agree that additional experimental data would strengthen the validation of the identified mutations. In response, we have indicated the ratio of wild-type to mutant parasites by Illumina NovaSeq6000 to validate the impact of the *Bg*ATP4 C-to-G and A mutations (Figure 2D).

> *Comment 2: Conducting an Ion Transport Assay is useful but has limitations. Non-specific binding or transport by other cellular components can lead to inaccurate results, causing false positives or negatives and making data interpretation difficult. Indirect measurements, like changes in fluorescence or electrical potential, can introduce artifacts. To improve accuracy, consider additional assays such as*
>
> *a. Radiolabeled Ion Flux Assay: tracks the movement of Na^+ using radiolabeled ions, providing direct evidence of ion transport.*
>
> *b. Electrophysiological Assay: measures ionic currents in real-time with patch-clamp techniques, offering detailed information about ATP4 activity.*

Thank you for highlighting the limitations of the ion transport assay and suggesting alternative approaches to improve accuracy. However, they require specialized equipment and expertise not currently available in our laboratory. We have acknowledged these limitations and included these alternative methods as part of the study's future directions. Thank you for your suggestions which will undoubtedly enhance the rigor and depth of our research.

Comment 3: *In-silico* predictions can provide plausible outcomes, but it is essential to evaluate how the recombinant purified protein and ligand interact and function at physiological levels. This aspect is currently missing and should be included. For example, incorporating immunoprecipitation and ATPase activity assays with both wild-type and mutant proteins, as well as detailed kinetic studies with Cipargamin, would be recommended to validate the findings of the study.

Thank you for your insightful suggestions regarding the validation of *in-silico* predictions. We recognize the importance of evaluating the interaction and function of recombinant purified proteins and ligands at physiological levels to strengthen the study's findings. (1) Incorporating experimental validation:

a. Immunoprecipitation assays: We agree that immunoprecipitation could provide valuable evidence of protein-ligand interactions. While this was not included in the current study due to limitations in sample availability, we plan to incorporate this assay in follow-up experiments.

b. ATPase activity assays: Assessing ATPase activity in both wild-type and mutant proteins is a crucial step in validating the functional impact of the identified mutations. We included the results in the revised manuscript (Figure 3H).

(2) Detailed kinetic studies with cipargamin: We appreciate the recommendation to conduct detailed kinetic analyses. These studies would provide deeper insights into the binding affinity and inhibition dynamics of cipargamin. We have included the results of these experiments in the current study (Figure 3I).

Comment 4: The study lacks specific suitable control drugs tested both *in vitro* and *in vivo*. For accurate drug assessment, especially when evaluating drugs based on a specific phenotype, such as enlarged parasites, it is important to use ATP4 gene-specific inhibitors. Including similar classes of drugs, such as Aminopyrazoles, Dihydroisoquinolines, Pyrazoleamides, Pantothenamides, Imidazolopiperazines (e.g., GNF179), and Bicyclic Azetidine Compounds, would provide more comprehensive validation.

Thank you for emphasizing the importance of including suitable control drugs. We acknowledge the absence of specific control drugs in the previous version of the manuscript. To date, no drug targeting ATP4 proteins in *Babesia* has been definitively identified. The suggested drugs could potentially disrupt the parasite's ability to regulate sodium levels by inhibiting *Pf*ATP4, a protein essential for its survival. This highlights *Pf*ATP4 as an attractive target for antimalarial drug development. However, further studies are required to evaluate whether these drugs exhibit similar activity against ATP4 homologs in *Babesia*.

> *Comment 5: Functional characterization of CIP through microscopic examination and quantification for assessing parasite size enlargement is not entirely reliable. A Flow Cytometry-Based Assay is recommended instead 9 along with suitable control antiparasitic drugs). To effectively monitor Cipargamin's action, conducting time-course experiments with 6-hour intervals is advisable rather than relying solely on endpoint measurements. Additionally, for accurate assessment of parasite morphology, obtaining representative qualitative images using Scanning Electron Microscopy (SEM) or*

> *Transmission Electron Microscopy (TEM) for treated versus untreated samples is recommended for precise measurements.*

Thank you for your constructive feedback regarding the methods for functional characterization of CIP and the evaluation of parasite morphology.

(1) Flow Cytometry-Based Assay: We agree that a flow cytometry-based assay would enhance the accuracy of detecting changes in parasite size and morphology. We will implement this method in future studies as our laboratory currently does not have the capability to conduct such experiments.

(2) Microscopy for Morphology Assessment: We acknowledge the importance of obtaining high-resolution, representative images of treated and untreated samples. Utilizing Scanning Electron Microscopy (SEM) or Transmission Electron Microscopy (TEM) for qualitative analysis will significantly improve the precision of our morphological assessments. However, both methods have limitations.

a. SEM: This technique can only scan the erythrocytes' surface; it cannot scan the parasite itself because it is inside the erythrocytes.

b. TEM: Since the parasite is fixed, observations from various angles may reveal longitudinal or cross-sectional portions, making it impossible to precisely view the parasite's dimensions. As a result, we employed TEM to precisely observe the parasite's internal structure alterations both before and after treatment, as seen in Figure 3C.

> *Comment 6: A notable contradiction observed is that mutant cells displayed reduced efficacy and affinity but more pronounced phenotypic effects. The BgATP4^{L921I} mutation shows a 2x lower susceptibility (IC_{50} of 887.9 ± 61.97 nM) and a predicted binding affinity of -6.26 kcal/mol with CIP. However, the phenotype exhibits significantly lower Na^+ concentration in BgATP4^{L921I} (P = 0.0087) (Figure 3E).*

The seemingly contradicting observation of reduced CIP binding and efficacy in the *Bg*ATP4^{L921I} mutant with a significant decrease in intracellular Na^+ concentration may be explained by factors other than the direct CIP interaction. Logically, we consider that CIP binds less effectively to its target in the *Bg*ATP4^{L921I} mutant, but the observed phenotype may be attributed to the functional consequences of the mutation. The *Bg*ATP4^{L921I} mutation probably directly impacts the function of *Bg*ATP4's ion transport mechanism, which likely disrupts Na^+ homeostasis independently. Thus, we hypothesize that the dysregulated Na^+ homeostasis is driven by the mutation itself rather than the already weakened inhibitory effect of CIP.

> *Comment 7: The manuscript does not clarify the percentage of mutations, and the number of sequence iterations performed on the ATP4 gene. It is also unclear whether clonal selection was carried out on the resistant population. If mutations are not present in 100% of the resistant parasites, please indicate the ratio of wild-type to mutant parasites and represent this information in the figure, along with the chromatograms.*

Thank you for your valuable comments. We appreciate your detailed observations and giving us the opportunity to clarify these points. During the long-term culture process, subculturing was performed every three days. Although clonal selection was not conducted, mutant strains were effectively selected during this process. Using the Illumina NovaSeq6000 sequencing platform, high-throughput next-generation sequencing was performed to detect ratio of wild-type to mutant parasites. Results showed that for *Bg*ATP4^{L921V}, 99.97% of 7,960 reads were G, and for *Bg*ATP4^{L921I}, 99.92% of 7,862 reads were A. To enhance clarity, we have included a

new figure (Figure 2D) illustrating the sequencing results. We believe this addition will help provide a clearer understanding for the readers.

> *Comment 8: While the compound's toxicity data is well-established, it is advisable to include additional testing in epithelial cells and liver-specific cell lines (e.g., HeLa, HCT, HepG2) if feasible for the authors. This would provide a more comprehensive assessment of the compound's safety profile.*

Thank you for your thoughtful suggestion. We included toxicity testing in human foreskin fibroblasts (HFF) as supplemental toxicity data to provide a more comprehensive evaluation of the compound's safety profile (Figure supplement 1B).

> *Comment 9: In the* in vivo *efficacy study, recrudescent parasites emerged after 8 days of treatment. Did these parasites harbor the same mutation in the ATP4 gene? The authors did not investigate this aspect, which is crucial for understanding the basis of recrudescence.*

Thank you for raising this important point. We acknowledge that understanding the genetic basis of recrudescence is critical for elucidating mechanisms of resistance and treatment failure. Although our current study did not include an analysis of the *Br*ATP4 gene in relapse parasites due to limitations in sample availability, we evaluated CIP efficacy in SCID mice and performed sequencing analysis of the *Bm*ATP4 gene in recrudescent samples. However, no mutation points were identified (Lines 211-212). We believe that if a relapse occurs after the 7-day treatment, it is unlikely that the parasites would easily acquire mutations.

> *Comment 10: The authors should explain their choice of BABL/c mice for evaluating CIP efficacy, as these mice clear the infection and may not fully represent the compound's effectiveness. Investigating CIP efficacy in SCID mice would be valuable, as they provide a more reliable model and eliminate the influence of the immune system. The rationale for not using SCID mice should be clarified.*

We appreciate the reviewer's suggestion regarding the use of SCID mice to evaluate the efficacy of CIP. In response to your suggestion, we have now included an experiment using SCID mice to evaluate the efficacy of CIP and to eliminate the confounding influence of the immune system. We further investigated the potential of combined administration of CIP plus TQ to eliminate parasites, as we are concerned that the long-term use of CIP as a monotherapy may be limited due to its potential for developing resistance. The results are shown in Figure 5C.

Comment 11: Do the *in vitro*-resistant parasites show any potential for cross-resistance with commonly used antiparasitic drugs? Have the authors considered this possibility, and what are their expectations regarding cross-resistance?

Thank you for your insightful question regarding the potential for cross-resistance between *in vitro*-resistant parasites and commonly used antiparasitic drugs. In response to your suggestion, we have now included experiments to assess whether *B. gibsoni* parasites that are resistant to CIP exhibit any cross-resistance to other commonly used antiparasitic drugs, such as atovaquone (ATO) and tafenoquine (TQ). The IC_{50} values for both ATO and TQ in the resistant strains showed only slight changes compared to the wild-type strain, with less than a onefold difference (Figure 5A, 5B). This minimal variation suggests that the resistant strain has a mild alteration in susceptibility to ATO and TQ, but not enough to indicate strong resistance or significant cross-resistance. This suggests that CIP could be used in combination with TQ to treat babesiosis.

> ***Reviewer #2 (Public review):***
>
> *Summary:*
>
> *In this manuscript, the authors have tried to repurpose cipargamin (CIP), a known drug against* plasmodium *and* toxoplasma *against* babesia*. They proved the efficacy of CIP on* babesia *in the nanomolar range.* In silico *analyses revealed the drug resistance mechanism through a single amino acid mutation at amino acid position 921 on the ATP4 gene of* Babesia*. Overall, the conclusions drawn by the authors are well justified by their data. I believe this study opens up a novel therapeutic strategy against babesiosis.*
>
> *Strengths:*
>
> *The authors have carried out a comprehensive study. All the experiments performed were carried out methodically and logically.*

Thank you for the comments and your time to review our manuscript.

> *Weaknesses:*
>
> *The introduction section needs to be more informative. The authors are investigating the binding of CIP to the ATP4 gene, but they did not give any information about the gene or how the ATP4 inhibitors work in general. The resolution of the figures is not good and the font size is too small to read properly. I also have several minor concerns which have been addressed in the "Recommendations for the authors" section.*

We thank the reviewer for their valuable comments. In response, we have revised the introduction to include a more detailed explanation of the ATP4 gene, its biological significance, and the mechanism of ATP4 inhibitors to provide a better context of the study (Lines 86-93). Additionally, we have reformatted the figures to enhance resolution and increased the font size to ensure improved readability. We also appreciate the reviewer's careful assessment of the manuscript and have addressed all minor concerns outlined in the "Recommendations for the Authors" section. A detailed, point-by-point response to each concern is provided in the response letter, and the corresponding revisions have been incorporated into the manuscript.

> ***Reviewer #3 (Public review):***
>
> *Summary:*
>
> *The authors aim to establish that cipargamin can be used for the treatment of infection caused by* Babesia *organisms.*
>
> *Strengths:*
>
> *The study provides strong evidence that cipargamin is effective against various* Babesia *species.* In vitro*, growth assays were used to establish that cipargamin is effective against* Babesia bovis *and* Babesia gibsoni*. Infection of mice with* Babesia microti *demonstrated that cipargamin is as effective as the combination of atovaquone plus azithromycin. Cipargamin protected mice from lethal infection with* Babesia rodhaini*. Mutations that confer resistance to cipargamin were identified in the gene encoding ATP4, a P-type* Na^+ *ATPase that was found in other apicomplexan parasites, thereby validating ATP4 as the target of cipargamin.*

We appreciate the reviewer for taking the time to review our manuscript.

> *Weaknesses:*
>
> *Cipargamin was tested* in vivo *at a single dose administered daily for 7 days. Despite the prospect of using cipargamin for the treatment of human babesiosis, there was no attempt to identify the lowest dose of cipagarmin that protects mice from* Babesia microti *infection. Exposure to cipargamin can induce resistance, indicating that cipargamin should not be used alone but in combination with other drugs. There was no attempt at testing cipargamin in combination with other drugs, particularly atovaquone, in the mouse model of* Babesia microti *infection. Given the difficulty in treating immunocompromised patients infected with* Babesia microti*, it would have been informative to test cipargamin in a mouse model of severe immunosuppression (SCID or rag-deficient mice).*

We thank the reviewer for raising these important comments. We address each concern as follows:

(1) Identifying the lowest protective dose of CIP:

Although our current study was designed to assess the efficacy of CIP at a single therapeutic dose over a 7-day period, we acknowledge that identifying the lowest effective dose would provide valuable information for optimizing treatment regimens. We plan to address this in future studies by conducting a dose-response experiment to identify the minimal protective dose of CIP.

(2) Testing CIP in combination with other drugs:

In the current study, we have tested the efficacy of tafenoquine (TQ) combined with CIP, as well as CIP or TQ administered individually, in a mouse model of *B. microti* infection. Our results demonstrated that, compared with monotherapy, the combination of CIP and TQ completely eliminated the parasites within 90 days of observation (Figure 5C).

(3) Testing in an immunocompromised mouse model:

We agree with the reviewer that evaluating CIP in immunocompromised models is critical for understanding its potential in treating immunocompromised patients. To address this, we have conducted experiments using SCID mice infected with *B. microti*. Our results indicated that the combination therapy of CIP plus TQ was effective in eliminating parasites in the severely immunocompromised model (Figure 5D).

> ***Recommendations for the authors:***
>
> ***Reviewer #1 (Recommendations for the authors):***
>
> *Comment 1: Table: Include the* in-silico *binding energies for each mutation and ligand.*

We have added binding energies for each mutation and ligand in Table supplement 3.

> *Comment 2: Did the authors investigate the potential of combination therapies involving CIP?*

We have tested the efficacy of TQ combined with CIP in a mouse model of *B. microti* infection.

> *Comment 3: Does this mutation affect the transmission of the parasite?*

Based on our observations, the growth and generation rates of the mutant strain are comparable to those of the wild-type strain. These findings suggest that the mutation does not

significantly affect the spread or transmission of the parasite. We have included this observation in the revised manuscript (Lines 243-244).

> *Comment 4: 60: Use abbreviations CLN for clindamycin and QUI for quinine.*

We have revised them accordingly (Lines 59-60).

> *Comment 5: 86: The hypothesis is not strong or convincing; it needs to be modified to be more specific and convincing.*

We have revised the hypothesis to reflect the rationale behind the study better and to support our claim more strongly (Lines 94-97).

> *Comment 6: 93: Change to: "*In vitro *efficacy of CIP against* B. bovis *and* B. gibsoni*.".*

We have changed the suggested content in the manuscript (Line 104).

> *Comment 7: 96: Define* CC_{50}.

We have added the definition of CC_{50} (Line 106).

> *Comment 8: 102: Change to: "...Balb/c mice increased dramatically in the...".*

We have changed the word following your recommendation (Line 114).

> *Comment 9: 108: "...significant decrease at 12 DPI...".*

We have revised it according to your suggestion (Line 120).

> *Comment 10: 110: "This indicates that the administration...".*

We have revised it according to your suggestion (Line 122).

> *Comment 11: Figure 1:*
>
> *(1) Panels A and B should clearly indicate parasite species within the graph for better self-explanation.*

We have indicated parasite species within the graph.

> *(2) For panels C, D, and E, if mice were eliminated or euthanized in the study, include a symbol in the graph to indicate this.*

For panels C and D, no mice were eliminated during the study; therefore, no symbol was added to these graphs. Panel F already provides information about the number of eliminated mice, which corresponds to the data in Panel E.

> *(3) In panels C, D, and E, use a continuation arrow for drug treatment rather than a straight line, to cover the duration of the treatment.*

We have updated the figures to use continuation arrows instead of straight lines to represent the duration of drug treatment.

> *Comment 12: Figure 2: The color combination for the WT and mutant curves is hard to read; consider using regular, less fluorescent, and more distinguishable colors.*

We have adjusted the color scheme to use more distinguishable and less fluorescent colors, ensuring better readability and clarity. The revised figure with the updated color scheme has been included in the updated manuscript, and we hope this resolves the readability concern.

> *Comment 13: Figure 3:*
>
> *(1) Panel A: Represent a single infected iRBC rather than a field for better visualization.*

We have updated Panel A to display a single infected iRBC instead of a field.

> *(2) Panels E and F: Change the color patterns, as the current colors, especially the green variants (WT and mutant L921V), are difficult to read.*

To improve readability, we have updated the color patterns for these panels by selecting more distinguishable colors with higher contrast (Figure 3F, 3G).

> *Comment 14: Figure 4: Panels B, C, and D: The text is too small to read; increase the font size or change the resolution.*

We have increased the font size and replaced the panels with high-resolution versions (Figure 4B, 4C, 4D).

> ***Reviewer #2 (Recommendations for the authors):***
>
> *Comment 1: In the last paragraph of the introduction, the authors mentioned determining the activity of CIP* in vitro *in* B. bovis *and* B. gibsoni *while* in vivo *in* B. microti *and* B. rodhaini*. It is not explained why they are testing the* in vitro *and* in vivo *effects on different* Babesia *species. Could you please add some logic there? Also, why did they mention measuring the inhibitory activity of CIP by monitoring the Na^+ and H^+ balance? This part needs to be rewritten with more information. The ATP4 gene is not properly introduced in the manuscript.*

We thank the reviewer for raising these important points. Below, we address each aspect of the comment in detail:

(1) Rationale for testing different *Babesia* spp. *in vitro* and *in vivo*:

B. bovis and *B. gibsoni* are well-established *Babesia* models for *in vitro* culture systems, allowing evaluation of CIP's inhibitory activity under controlled laboratory conditions. *B. microti* and *B. rodhaini*, on the other hand, are commonly used rodent models for the *in vivo* studies of babesiosis, enabling the assessment of drug efficacy in a mammalian host system. This multi-species approach provides a comprehensive evaluation of CIP's efficacy across *Babesia* spp. with different biological characteristics.

(2) Measuring CIP's inhibitory activity via Na^+ and H^+ balance:

We acknowledge that this section of the introduction requires more context. The revised manuscript now includes additional information explaining that the ATP4 gene, which encodes a Na^+/H^+ transporter, is the proposed target of CIP (Lines 86-93). CIP disrupts the ion homeostasis maintained by ATP4, leading to an imbalance in Na^+ and H^+ concentrations. Monitoring these ionic changes provides a mechanistic understanding of CIP's mode of action

and its impact on parasite viability. This rationale has been expanded in the introduction to clarify its significance.

> *Comment 2: The figure fonts are too small. The resolution for the images is also poor.*

We have increased the font size in all figures to improve readability. Additionally, we have replaced the figures with high-resolution versions to ensure clarity and visual quality.

> *Comment 3: Figures 1A and 1B: one of the error bars merged to the X-axis legend. Please modify these panels. Which curve was used to determine the IC_{50} values (although it's mentioned in the methods section, would it be better to have the information in the figure legends as well)?*

We thank the reviewer for their comments regarding Figures 1A and 1B.

(1) Error bars overlapping the X-axis legend:

The error bars in the figures were automatically generated using GraphPad Prism9 based on the data and are determined by the values themselves. Unfortunately, this overlap cannot be avoided without altering the data representation.

(2) IC_{50} curve information:

To clarify the determination of IC_{50} values, we have already included gray dashed lines in the graphs to indicate where the IC_{50} values were derived from the curves. This visual representation provides clear information about the IC_{50} points.

> *Comment 4: Supplementary Figure 1: what are MDCK cells? What is CC_{50}? Please mention their full forms in the text and figure legends (they should be described here because the methods section comes later). What is meant by a predicted selectivity index? There should be an explanation of why and how they did it. Which curve was used to determine the IC_{50} values?*

We thank the reviewer for pointing out the need to clarify terms and provide additional context in the supplementary figure and text. We have updated the figure legend and text to include the full forms of MDCK (Madin-Darby canine kidney) cells and CC_{50} (50% cytotoxic concentration), ensuring clarity for readers encountering these terms for the first time. In text, now we have included a brief explanation of the selectivity index as a measure of a drug's safety and specificity (Lines 108-110). The selectivity index is calculated as the ratio between the half maximal inhibitory concentration (IC_{50}) and the 50% cytotoxic concentration (CC_{50}) values (Lines 333-335). We also have already included gray dashed lines in the graphs to indicate where the IC_{50} values were derived from the curves (Figure supplement 1).

> *Comment 5: Figures 1C-F: It feels unnecessary to write down n=6 for each panel and each group. Since "n" is equal for all, it would be nice to just mention it in the figure legend only.*

We appreciate the reviewer's suggestion regarding the notation of "n=6" in Figures 1C-F. To improve clarity and reduce redundancy, we have removed the "n=6" notation from the individual panels and included it in the figure legend instead.

> *Comment 6: Figure 2A: was never mentioned in the text.*

We have described the sequencing results for the wild-type *B. gibsoni* ATP4 gene with a reference to Figure 2A in the revised manuscript (Lines 134-135).

> *Comment 7: Figure 2D: some of the error bars merged to the X-axis legend. Please modify. Again, which curve was used to determine the IC_{50} values? Can the authors explain why the pH declined after 4 minutes?*

We thank the reviewer for this insightful question.

(1) Error bars overlapping the X-axis legend:

The error bars in Figure 2E were automatically generated using GraphPad Prism9 and are determined by the underlying data values. Unfortunately, this overlap cannot be avoided without altering the data representation.

(2) IC_{50} curve information:

Since Figure 2E contains three separate curves, adding dashed lines to indicate the IC_{50} for each curve would make the figure overly cluttered and reduce readability. To address this, we have clearly indicated the IC_{50} values in Figures 1A and 1B and described the methodology for determining IC_{50} values in the Methods section. We believe this approach provides sufficient clarity without compromising the visual experience of Figure 2E.

(3) The pH decline observed after 4 minutes (Figure 3E) may be attributed to the following factors:

a. Ion transport dynamics:

The initial rise in pH likely reflects the rapid inhibition of Na^+/H^+ exchange mediated by CIP, which temporarily alkalinizes the intracellular environment. However, after this initial phase, compensatory mechanisms, such as proton influx or metabolic acid production, may lead to a subsequent decline in pH.

b. Drug kinetics and target interaction:

The decline could also result from the time-dependent effects of CIP on ATP4-mediated ion transport. As the drug action stabilizes, the parasite may partially restore ionic balance, leading to a decrease in intracellular pH.

> *Comment 8: Supplementary Figure 2: It's difficult to distinguish between red and pink colors, so it would be wise to use two contrasting colors to distinguish between* Pf *and* Tg *CIP resistant cites.*

We have updated the figure to enhance clarity. Purple squares and arrows now represent sites linked to *P. falciparum* CIP resistance, replacing the previous red squares. Similarly, gray squares and arrows have replaced the green squares to denote sites associated with *T. gondii* (Figure supplement 2).

> *Comment 9: Line 65: Is it possible to add a reference here?*

We have added a reference in line 65.

> *Comment 10: Line 69: Please spell the full form of G6PD as it was never mentioned before.*

We have added the full form of G6PD in lines 69-70.

> *Comment 11: Line 103: mention what DPI is (irrespective of the methods section which comes later).*

We have spelled out DPI (days postinfection) in line 115.

> *Comment 12: Line 120: It's not explained why* B. gibsoni *ATP4 gene was investigated? There should be more explanation and references to previous work.*

We thank the reviewer for pointing out the need to provide more context for investigating the *B. gibsoni* ATP4 gene. To address this, we have added more information to the introduction, explaining that the ATP4 gene, which encodes a Na^+/H^+ transporter, is the proposed target of CIP (Lines 86-93).

> *Comment 13: Line 203-219: line spacing seems different from the rest of the manuscript.*

We have corrected the incorrect format (Lines 262-278).

> ***Reviewer #3 (Recommendations for the authors):***
>
> *Comment 1: Lines 66-68: The report by Marcos et al. 2022 did not demonstrate that tafenoquine was effective in curing relapsing babesiosis. In the discussion of that article, the authors state that "it is impossible to conclude that the drug tafenoquine provided any clinical benefit." The first demonstration of tafenoquine efficacy against relapsing babesiosis was reported by Rogers et al. 2023 and confirmed by Krause et al. 2024. Please rephrase the statement and use relevant citations.*

We thank the reviewer for pointing out this issue and we have rephrased the statement and used relevant citations (Lines 66-68).

> *Comment 2: Line 103: mean parasitemia at 10 DPI is reported to be 35.88% but Figure 1C appears to indicate otherwise.*

We are sorry for the carelessness, the correct mean parasitemia at 10 DPI is 38.55%, and this has been updated in line 115 of the revised manuscript to reflect the data shown in Figure 1C.

> *Comment 3: Line 116: parasitemia is said to recur on day 14 post-infection but Figure 1E indicates that recurrence was already noted on day 12 post-infection.*

We thank the reviewer for pointing out this inconsistency. We have corrected the relapse day to reflect that recurrence was noted on day 12 post-infection, as shown in Figure 1E. This correction has been made in the revised manuscript (Line 128).

> *Comment 4: Line 120: Replace "wells" with "strains". Also, start the paragraph with one brief sentence to state how resistant parasites were generated.*

We have replaced "wells" with "strains" and added one brief sentence to explain how resistant parasites were generated (Lines 132-134).

> *Comment 5: Line 169: is Ji et al, 2022b truly the appropriate reference to support a statement on tafenoquine?*

We thank the reviewer for highlighting this point. We have added one other reference to support a statement on tafenoquine. The IC_{50} value of TQ was 20.0 ± 2.4 μM against *B. gibsoni*

(Ji et al., 2022b), and 31 μM against *B. bovis* (Carvalho et al., 2020) (Lines 223-225).

> *Comment 6: Lines 184-185: given that exposure to CIP induces mutations in the ATP4 gene and therefore resistance to CIP, what is the prospect of using CIP for the treatment of babesiosis? Can the authors speculate on whether CIP should not be used alone but rather in combination with other drugs currently used for the treatment of human babesiosis?*

We thank the reviewer for raising this important question. Given that exposure to CIP induces mutations in the ATP4 gene, leading to resistance, we acknowledge that the long-term use of CIP as a monotherapy may be limited due to the potential for resistance development. To address this concern, we investigated the combination therapy of TQ and CIP to achieve the complete elimination of *B. microti* in infected mice (a model for human babesiosis). The results of this study are presented in Figure 5C.

> *Comment 7: Lines 258-259: it is stated that drug treatment was initiated on day 4 post-infection when mean parasitemia was 1% and that drug treatment was continued for 7 days. This is not the case for* B. rodhaini *infection. As reported in Figure 1E, treatment was initiated on day 2 post-infection.*

We apologize for the oversight and any confusion caused. We have corrected the statement to reflect that drug treatment for *B. rodhaini*-infected mice was initiated at 2 DPI, as reported in Figure 1E (Lines 347-349).

> *Comment 8: Lines 282-285: RBCs are said to be exposed to CIP for 3 days but parasite size is said to be measured on day 4. Which is correct?*

We thank the reviewer for pointing out this discrepancy. To clarify, the infected erythrocytes were exposed to CIP for three consecutive days (72 hours). Blood smears were then prepared at the 73rd hour, corresponding to the fourth day.

> *Comment 9: Lines 35-37: this sentence can be omitted from the abstract as it does not summarize additional insight or additional data.*

We have omitted this sentence from the abstract.

Comment 10: Line 55: replace Drews et al. 2023 with Gray and Ogden 2021 (doi: 10.3390/pathogens10111430). This excellent article directly supports the statement made by the authors.

We appreciate the reviewer's suggestion and have replaced the reference with Gray and Ogden, 2021 (doi: 10.3390/pathogens10111430) (Line 54).

> *Comment 11: Line 55: modify the start of sentence to read "The disease is known as babesiosis ...".*

We have modified the sentence (Line 54).

> *Comment 12: Line 56: rephrase to read ".... but chronic infections can be asymptomatic".*

We have modified the sentence (Line 55).

> *Comment 13: Line 57: rephrase to read "The fatality rate ranges from 1% among all cases to 3% among hospitalized cases but has been as high as 20% in immunocompromised patients."*

We have rephrased the sentence (Lines 55-57).

> *Comment 14: Line 61: replace Holbrook et al. 2023 with Krause et al. 2021 (doi: 10.1093/cid/ciaa1216).*

We have replaced Holbrook et al. 2023 with Krause et al. 2021 (doi: 10.1093/cid/ciaa1216) (Line 60).

> *Comment 15: Line 62: rephrase to read "... cytochrome b, which is targeted by atovaquone, were identified in patients with relapsing babesiosis." Here, also cite Lemieux et al., 2016; Simon et al., 2017; Rosenblatt et al, 2021, Marcos et al., 2022; Rogers et al., 2023; Krause et al., 2024.*

We have rephrased the sentence and cited the suggested references (Lines 61-64).

> *Comment 16: Line 65: rephrase "Despite its efficacy, this combination can elicit adverse drug reactions (Vannier and Krause, 2012)."*

We have rephrased the sentence (Lines 65-66).

> *Comment 17: Lines 75-77: rephrase to read "... of the drug indicated that CIP taken orally had good absorption, a long half-life, and ...".*

We have rephrased the sentence (Lines 76-77).

> *Comment 18: Line 79: remove "the".*

We have removed "the" (Lines 79-80).

> *Comment 19: Lines 83-85: rephrase to read "Mice infected with* T. gondii *that were treated with CIP on the day of infection and the following day had 90% fewer parasites 5 days post-infection (Zhou et al., 2014).".*

We have rephrased the sentence (Lines 83-85).

> *Comment 20: Line 90: shorten the sentence to end as follows "... of CIP on* Babesia *parasites.".*

We have shortened the sentence in line 100 with your suggestion.

> *Comment 21: Line 96: spell out CC_{50}.*

We have spelled out the full form of CC_{50} (Line 106).

> *Comment 22: Line 104: remove "of body weight".*

We have removed "of body weight" (Line 116).

> *Comment 23: Line 108: delete "from 8 DPI to 24 DPI, with statistically significant decreases".*

We have deleted "from 8 DPI to 24 DPI, with statistically significant decreases" (Line 120).

> *Comment 24: Line 111: start a new paragraph with the sentence "BALB/c mice infected ...".*

We have started a new paragraph with the sentence "BALB/c mice infected ..." (Line 124).

> *Comment 25: Line 123: replace "showed" with "occurred".*

We have replaced "showed" with "occurred" (Line 138).

> *Comment 26: Line 127: rephrase to read "... sensitivity of the resistant parasite lines ...".*

We have rephrased the sentence (Line 144).

> *Comment 27: Lines 137-140: rephrase to read ".... lines were lower when compared with ..." .*

We have rephrased the sentence (Line 158).

> *Comment 28: Line 149: replace "BgATP4" with "*B. gibsoni *ATP4".*

We have replaced "*Bg*ATP4" with "*B. gibsoni* ATP4" (Line 183).

> *Comment 29: Line 154: spell out "pLDDT" prior to pLDDT.*

We have provided the full form of pLDDT in the revised manuscript (Line 188).

> *Comment 30: Lines 165-166: rephrase to read "CIP is a novel compound that inhibits* Plasmodium *development by targeting ATP4 and has been ...".*

We have rephrased the sentence (Lines 219-220).

> *Comment 31: Lines 171-172: rephrase to read "...AZI, the combination recommended by the CDC in the United States.*

We have rephrased the sentence (Lines 226-227).

> *Comment 32: Line 173: rephrase to read "...* B. rodhaini *infection, with survival up to 67%.".*

We have rephrased the sentence (Line 228).

> *Comment 33: Lines 175-178: rephrase to read "In a previous study, a* P. falciparum *Dd2 strain that acquired resistance to CIP carried the G358S mutation in the ...".*

We have rephrased the sentence (Lines 230-231).

> *Comment 34: Lines 179-180: rephrase to read "ATP4 is found in the parasite plasma membrane and is specific to the subclass of apicomplexan parasites.".*

We have rephrased the sentence (Lines 232-233).

> *Comment 35: Lines 182-184: rephrase to read "In another study of* Toxoplasma gondii*, a cell line that carried the mutation G419S in the TgATP4 gene was 34 times ...".*

We have rephrased the sentence (Lines 235-237).

> *Comment 36: Lines 201-202: deleted the last sentence of this paragraph.*

We have deleted the last sentence of the paragraph (Line 261).

> *Comment 37: Line 228: rephrase to read "... that CIP had a weaker binding to BgATP4^{L921I} than to BgATP4^{L921V}.".*

We have rephrased the sentence (Lines 294-295).

> *Comment 38: Lines 261-262: please state that drugs were prepared in sesame oil. Add "20 mg/kg" in front of AZI.*

We have stated that drugs were prepared in sesame oil and added "20 mg/kg" in front of AZI (Lines 350-352).

> *Comment 39: Line 265: replace "care" with "treatments".*

We have replaced "care" with "treatments" (Line 355).

> *Comment 40: Line 267: replace "observe" with "assess".*

We have replaced "observe" with "assess" (Line 357).

> *Comment 41: Lines 269-271: please provide the absolute numbers of* B. gibsoni *infected RBCs and the absolute numbers of uninfected RBCs that were added to the culture medium.*

We thank the reviewer for this suggestion. In the revised manuscript, we have included the absolute numbers of *B. gibsoni*-infected RBCs and uninfected RBCs added to the culture medium. Specifically, the culture medium contained 10 μL (5×10^{6}) *B. gibsoni* iRBCs mixed with 40 μL (4×10^{8}) uninfected RBCs (Lines 360-361).

> *Comment 42: Line 279: replace "confirmed" with "identified".*

We have replaced "confirmed" with "identified" (Line 370).

> *Comment 43: Figure Supplement 2: the squares are not readily visible. Could the entire column corresponding to the mutation position be highlighted?*

We thank the reviewer for this suggestion. To improve visibility, we have changed the color of the squares and added arrows to make the mutation sites as prominent as possible. Unfortunately, due to software limitations, we were unable to highlight the entire column corresponding to the mutation position.

> *Comment 44: Figure Supplement 4: for the parasite that carries a mutation in BgATP4, please delete the arrows that are next to BgATP4. These arrows send the message that the mutation ATP4 has an active role in pumping back Na^{+} and H^{+} back in their compartment, which is not the case.*

We thank the reviewer for their observation. The dotted arrows next to *Bg*ATP4 are intended to indicate the recovery of H^{+} and Na^{+} balance facilitated by the mutated ATP4, which

reduces susceptibility to ATP4 inhibitors. To avoid potential confusion, we have revised the figure legend to clearly explain the role of the arrows, ensuring the intended message is accurately conveyed.

https://doi.org/10.7554/eLife.101128.2.sa0